Arctic Ocean and Hudson Bay Freshwater Exports: New Estimates from 7 Decades of Hydrographic Surveys on the Labrador Shelf

CRISTIAN FLORINDO-LÓPEZ, SHELDON BACON, YEVGENY AKSENOV

National Oceanography Centre, Southampton, United Kingdom

LÉON CHAFIK

Department of Meteorology and Bolin Centre for Climate Research, Stockholm University, Stockholm, Sweden

EUGENE COLBOURNE

Fisheries and Oceans Canada, Northwest Atlantic Fisheries Centre, St. John's, NL, Canada

N. PENNY HOLLIDAY

National Oceanography Centre, Southampton, United Kingdom

Corresponding author address: Cristian Florindo-Lopez, Marine Physics and Ocean Climate Group, National Oceanography Centre, Southampton SO14 3ZH, U.K.
Email: criflor@noc.ac.uk

Early Online Release: This preliminary version has been accepted for publication in *Journal of Climate*, may be fully cited, and has been assigned DOI 10.1175/JCLI-D-19-0083.1. The final typeset copyedited article will replace the EOR at the above DOI when it is published.

© 2020 American Meteorological Society

Downloaded from http://journals.ametsoc.org/jcli/article-pdf/doi/10.1175/JCLI-D-19-0083.1/4954456/jclid190083.pdf by UNIVERSITY OF SOUTHAMPTON HIGHFIELD user on 11 June 2020

ABSTRACT

While reasonable knowledge of multi-decadal Arctic freshwater storage variability exists, we have little knowledge of Arctic freshwater exports on similar timescales. A hydrographic time series from the Labrador Shelf, spanning seven decades at annual resolution, is here used to quantify Arctic Ocean freshwater export variability west of Greenland. Output from a high-resolution coupled ice-ocean model is used to establish the representativeness of those hydrographic sections. Clear annual to decadal variability emerges, with high freshwater transports during the 1950s and 1970s–80s, and low transports in the 1960s, and from the mid-1990s to 2016, with typical amplitudes of 30 mSv (1 Sv = 10^6 m^3 s^{-1}). The variability in both the transports and cumulative volumes correlates well both with Arctic and North Atlantic freshwater storage changes on the same timescale. We refer to the "inshore branch" of the Labrador Current as the Labrador Coastal Current, because it is a dynamically- and geographically-distinct feature. It originates as the Hudson Bay outflow, and preserves variability from river runoff into the Hudson Bay catchment. We find a need for parallel, long-term freshwater transport measurements from Fram and Davis Straits, to better understand Arctic freshwater export control mechanisms and partitioning of variability between routes west and east of Greenland, and a need for better knowledge and understanding of year-round (solid and liquid) freshwater fluxes on the Labrador shelf. Our results have implications for wider, coherent atmospheric control on freshwater fluxes and content across the Arctic and northern North Atlantic Oceans.

Downloaded from http://journals.ametsoc.org/jcli/article-pdf/doi/10.1175/JCLI-D-19-0083.1/4954456/jclid190083.pdf by UNIVERSITY OF SOUTHAMPTON HIGHFIELD user on 11 June 2020

Accepted for publication in *Journal of Climate*. DOI10.1175/JCLI-D-19-0083.1.

1. Introduction

The North Atlantic Ocean is important both to regional and to global climate variability on multi-decadal timescales: as heat is released near-surface at high latitudes from ocean to atmosphere, water becomes denser, sinks, and closes the Meridional Overturning Circulation by returning south at depth, as popularised by Broecker (1991). In high latitudes, density is mainly controlled by salinity (Carmack, 2007), and it has long been recognised that dense water formation rates are sensitive to freshwater inputs by their impact on stratification (Manabe and Stouffer, 1995). Knowledge of freshwater fluxes into the North Atlantic remains essential to understanding the overturning circulation.

The Arctic Ocean is a substantial freshwater reservoir, receiving inputs from precipitation, oceanic inflows and river and melt-water run-off. It is a source of freshwater, which is exported to the subpolar North Atlantic (Carmack 2000; Haine et al., 2015; Carmack et al., 2016). The Arctic Ocean freshwater export rate is substantially modulated by changing internal rates of freshwater storage and release, and is known to vary on decadal timescales and longer (Polyakov et al. 2008). Over the past two decades it has been increasing by 600±300 km^3 yr^{-1} (Rabe et al. 2014).

Partly as a consequence of Arctic Ocean exports, the northern North Atlantic freshwater budget also varies on decadal timescales and is characterised by periodic dilution events (Curry and Mauritzen 2005). Periods of unusually low salinity in the 1970s, 1980s and 1990s have been called "Great Salinity Anomalies" (Dickson et al. 1988, Belkin et al. 1998, Belkin 2004), and have been explained as the result of anomalously high Arctic freshwater exports, whether ice (Häkkinen and Proshutinsky 2004) or liquid (Karcher et al. 2005), and periods of lower Arctic salinity are associated with a saltier North Atlantic (Peterson et al. 2006). Sundby and Drinkwater (2007) associate periods of both positive and negative salinity

Downloaded from http://journals.ametsoc.org/jcli/article-pdf/doi/10.1175/JCLI-D-19-0083.1/4954456/jclid190083.pdf by UNIVERSITY OF SOUTHAMPTON HIGHFIELD user on 11 June 2020

Accepted for publication in *Journal of Climate*. DOI10.1175/JCLI-D-19-0083.1.

anomalies with varying seawater volume fluxes in and out of the Arctic Ocean. Thus the Arctic and Atlantic freshwater budgets are linked.

There is now a large and growing body of knowledge quantifying multi-decadal, interannual and even seasonal changes in freshwater storage in the Arctic (Polyakov et al. 2008, Giles et al. 2012, Polyakov et al. 2013, Rabe et al. 2014, Proshutinsky et al. 2015, Armitage et al. 2016), reinforced by understanding of regional changes in wind forcing that cause ocean spin-up and spin-down, particularly of the Beaufort Gyre, that lead to increased freshwater restraint within, or release from, the Arctic Ocean (Proshutinsky and Johnson 1997, Häkkinen and Proshutinsky 2004, Köberle and Gerdes 2007, Proshutinsky et al. 2009, Lique et al. 2009, Giles et al. 2012, Rabe et al. 2014, Proshutinsky et al. 2015), with increasing understanding of the role of changing sea ice conditions in modulating ocean spin-up and spin-down (Giles et al. 2012, Tsamados et al. 2014, Martin et al. 2016).

We know that the freshwater budgets of the Arctic and Atlantic Oceans are related on decadal timescales (Proshutinsky et al. 2002, Peterson et al. 2006), and we are interested to learn whether freshwater storage changes in the two oceans are reflected in inter-ocean freshwater flux changes. For example, we might expect that an increase in Arctic freshwater storage would correspond to a restraint in Arctic freshwater export, and therefore to a decrease in Atlantic freshwater storage, and vice-versa. However, while long-term observations now exist at both main Arctic export gateways (Fram Strait: Rabe et al. 2013; Davis Strait: Curry et al. 2014), and balanced pan-Arctic freshwater budgets are beginning to emerge (Tsubouchi et al. 2012, 2018), those observations do not yet capture multi-decadal variability. Therefore quantification of links between variations in freshwater storage and fluxes remains elusive (cf. Haine et al. 2015).

Downloaded from http://journals.ametsoc.org/jcli/article-pdf/doi/10.1175/JCLI-D-19-0083.1/4954456/jclid190083.pdf by UNIVERSITY OF SOUTHAMPTON HIGHFIELD user on 11 June 2020

Accepted for publication in *Journal of Climate*. DOI10.1175/JCLI-D-19-0083.1.

The impact of Arctic storage changes on oceanic freshwater export, the separation of the export into the pathways east and west of Greenland by which it reaches the North Atlantic, and the relative importance of liquid (seawater) versus solid (sea ice) phases remain unclear. For example, Häkkinen (1993) and Karcher et al. (2005) attribute the Great Salinity Anomaly (Dickson et al. 1988) to the export of sea ice through Fram Strait, east of Greenland. Karcher et al. (2005) also describe the importance of the export west of Greenland to a 1990s North Atlantic low salinity event. Prinsenberg and Hamilton (2005) observed the export through the Canadian Arctic Archipelago to be the largest sink of Arctic liquid freshwater. Lique et al. (2009) suggested in a model study that there may be countervailing changes in freshwater export between east and west sides of Greenland, but as yet there is no supporting observational evidence (see also Aksenov et al. 2010).

Our aim in this study is to determine whether a multi-decadal record of seawater properties on and near the eastern Canadian (Labrador) shelf can be used to generate new knowledge of Arctic freshwater exports west of Greenland. It has long been known (Smith et al. 1937; Kollmeyer et al. 1967) that the seas off the Labrador coast are comprised of three components: the recirculating West Greenland Current, the cold Arctic waters of the Baffin Island Current, and the fresh outflow from Hudson Bay through Hudson Strait. With these three sources, the naming convention of the "Labrador Current" is an over-simplification, so we refer below instead to the Labrador Current System.

Perhaps the best-known feature of the Labrador Current System is the Cold Intermediate Layer (CIL; Petrie et al. 1988), in which the cold and relatively fresh waters overlying the eastern Canadian continental shelf are capped in summer by a thin, seasonal, warm layer, and are separated from the warmer, higher-density waters of the continental slope region by a strong density front. The CIL is present in all years and throughout most (or all) of the year. Its cross-sectional area (or regional volume), bounded by the 0 ºC isotherm, is regarded as a robust

Downloaded from http://journals.ametsoc.org/jcli/article-pdf/doi/10.1175/JCLI-D-19-0083.1/4954456/jclid190083.pdf by UNIVERSITY OF SOUTHAMPTON HIGHFIELD user on 11 June 2020

Accepted for publication in *Journal of Climate*. DOI10.1175/JCLI-D-19-0083.1.

index of regional ocean climate conditions. Significant interannual variability in the area of the CIL is highly coherent from the Labrador Shelf to the Grand Banks. Colbourne et al. (1995) quantified its area using three different isotherms (–1, 0 and 1 ºC), and although the average area varied with definition, the interannual variability remained relatively insensitive. Annual updates of the CIL time series are available in the International Council for the Exploration of the Sea Report on Ocean Climate – https://ocean.ices.dk/iroc/.

From this position, the paper is structured as follows. Having presented our data, model and methods (Section 2), we then use our model to refine our understanding of the Labrador Current System (section 3). We apply the new understanding to our data in section 4, and in section 5 we summarise and discuss future prospects.

2. Data, Model and Methods

The physical properties of the seas off Labrador and Newfoundland have been studied since the early 20th Century (Colbourne 2004). The first observations of the Labrador Current were carried out by the *Marion* and *General Green* expeditions from 1928 to 1935 (Smith et al. 1937) in support of the International Ice Patrol that was formed in 1913 and carried out by the US Coast Guard. Since the early 1950s, most regional ocean measurements were carried out along standardized stations and sections by the International Commission for the Northwest Atlantic Fisheries in support of fish stock assessment (Templeman 1975). In this study we focus on one particular section – the Seal Island section (Colbourne et al. 1995).

We choose the Seal Island section because is the northernmost of the standard sections. It extends from the Labrador coast across the shelf break and into the deep Labrador Sea (Figure 1). While measurements in the vicinity of the Seal Island section exist from the 1920s, we choose to begin at 1950, when the number and location of section stations was first standardarised. Therefore we analyse sections occupied between 1950 and 2016 (inclusive),

Downloaded from http://journals.ametsoc.org/jcli/article-pdf/doi/10.1175/JCLI-D-19-0083.1/4954456/jclid190083.pdf by UNIVERSITY OF SOUTHAMPTON HIGHFIELD user on 11 June 2020

Accepted for publication in *Journal of Climate*. DOI10.1175/JCLI-D-19-0083.1.

one section per year, from the summertime occupation (made in July or August), which has the longest continuous record: 60 of those 67 years provide useful temperature and salinity measurements. Records are available from other months in the calendar year, but they are shorter and/or discontinuous. This approach also avoids any aliasing of the seasonal cycle. For reference we show the full data distribution by year and month in Figure S1.

The Seal Island section originally comprised 9 standard stations. All profiles originally measured temperature by reversing thermometer; some also measured salinity by titration. The section was extended to 14 stations (Table A1, Figure 1) from 1993, by which time, measurements were made electronically by CTD, the instrument that measures continuous profiles of conductivity (and hence salinity), temperature and depth. The data accuracy, their temporal and geographical distribution, and our quality control procedure are described in Appendix A. Figure 2 (a–d) shows mean sections of temperature, salinity, density and geostrophic velocity (referenced to zero at the bottom) for summertime (July–August) 1995-2010, where the date range is chosen for comparison with model means in section 3 below. Figure S2 shows decadal mean property sections spanning 1950-2016, for reference. The temperature section is characterised by a warm surface layer (up to 8 °C) and a subsurface minimum (<0 °C: the CIL) that stretches from the coast (at 0 km on the section) to the shelf edge at ~200 km, while offshore, the water is warmer (3-4°C) and more uniform below the surface. Salinity has a different structure to temperature. Close to the coast, sloping isohalines form a fresher (<32.5), wedge-shaped feature that is thickest next to the coast and tapers offshore. The fresh surface layer (<20 m) reaches as far east as the shelf edge at ~200 km from the coast. Over most of the shelf the isohalines are fairly horizontal; salinity increases to 34 at the seafloor. At ~200–250 km a strong salinity front means the isohalines rapidly shoal before flattening at 20–40 m, with typical surface values of 32-33. Salinity is an order of magnitude more important than temperature for the control of density over the

Accepted for publication in *Journal of Climate*. DOI10.1175/JCLI-D-19-0083.1.

Downloaded from http://journals.ametsoc.org/jcli/article-pdf/doi/10.1175/JCLI-D-19-0083.1/4954456/jclid190083.pdf by UNIVERSITY OF SOUTHAMPTON HIGHFIELD user on 11 June 2020

Labrador shelf (Figure 2): a temperature range of 6 ºC equates to ~0.6 kg m^{-3} in density, while a salinity range of 6 equates to ~5 kg m^{-3} in density. Temperature is still a valuable water mass tracer.

The Nucleus for European Modelling of the Ocean (NEMO) is a widely-used framework for oceanographic modelling that performs well in the northern high latitudes: e.g. Jahn et al. (2012), Lique and Steele (2012), Bacon et al. (2014), Marzocchi et al. (2015), Aksenov et al. (2016). NEMO uses the primitive equation model Ocean Parallelisé (OPA 9.1; Madec and the NEMO team 2016) coupled with the Louvain-la-Neuve sea ice model (LIM2; Fichefet and Morales Maqueda 1997). The sea ice model uses Elastic-Viscous-Plastic rheology (Hunke and Dukowicz 1997) with numerical implementation on a C-grid (Bouillon et al. 2009). The ocean model is discretised on a tri-polar C-grid with two northern poles (in Siberia and Canada) and the geographical South Pole. Its bathymetry is derived from the ETOPO2v2 global relief Earth Topography (National Geophysical Data Center 2006), with patches from the International Bathymetric Chart of the Arctic Ocean (Jakobsson et al. 2008) in the Arctic. In the deep ocean the model bathymetry utilises the Smith and Sandwell (1997, 2004) 1/2 minute-resolution database, which is derived from a combination of satellite altimeter data and shipboard soundings and is continuously updated. For the continental shelves the model bathymetry is updated from the General Bathymetric Chart of the Oceans (e.g. Becker et al. 2009) dataset.

The ocean model solves the Navier-Stokes equations using the Boussinesq approximation, in which density is considered constant and is called the reference density (ρ_0), except when solving the hydrostatic balance equation. In the Boussinesq approximation, mass conservation reduces to the incompressibility equation, so that the model conserves volume (considered also as Boussinesq mass, which is a product of volume and ρ_0) rather than mass.

Downloaded from http://journals.ametsoc.org/jcli/article-pdf/doi/10.1175/JCLI-D-19-0083.1/4954456/jclid190083.pdf by UNIVERSITY OF SOUTHAMPTON HIGHFIELD user on 11 June 2020

Accepted for publication in *Journal of Climate*. DOI10.1175/JCLI-D-19-0083.1.

The horizontal momentum balance is also approximated with constant ρ_0. The hydrostatic balance, described by Madec and the NEMO team (2016), uses *in-situ* density in a formulation originally due to Jackett and McDougall (1995).

The model configuration used in the present analysis is ORCA0083 with 1/12° mean horizontal resolution. NEMO's tripolar grid amplifies resolution in high latitudes, to ca. 5 km in the Labrador Sea (ORCA0083), so that it is eddy-permitting on the Labrador shelves and eddy-resolving in the Labrador Sea (Nurser and Bacon 2014). In the vertical, the model contains 75 levels from the surface to 5900 m, and layers increase in thickness from 1 m at the surface to 204 m at the bottom; 29 levels cover the first 150 m. Partial steps in the model bottom topography are used to improve model approximation of steep seabed relief near continental shelves (Barnier et al. 2006). The ocean free surface is non-linear in ORCA0083 (Levier et al. 2007). An iso-neutral Laplacian operator is used for lateral tracer diffusion. A bi-Laplacian horizontal operator is applied for momentum diffusion. A turbulent kinetic energy closure scheme is used for vertical mixing. To address shallow seasonal biases in the mixed layer depth simulations, the turbulent kinetic energy scheme has been modified, accounting for mixing caused by surface wave breaking, Langmuir circulation and mixing below the mixed layer due to internal wave breaking. To improve stability of the temperature and salinity advection, a total variance dissipation advection scheme is implemented in the model; see Madec and NEMO System Team (2016) for details.

The ORCA0083 model run starts in 1978 from climatological conditions that combine the World Ocean Atlas (Levitus 1989) with the Polar Hydrographic Climatology (Steele et al. 2001), with ocean time step 200 s and atmospheric forcing fields obtained from the DRAKKAR Forcing Set (DFS4.1) reanalysis (Brodeau et al. 2010). The sea surface salinity is relaxed toward the monthly mean from the World Ocean Atlas, which has a resolution of 1°

Downloaded from http://journals.ametsoc.org/jcli/article-pdf/doi/10.1175/JCLI-D-19-0083.1/4954456/jclid190083.pdf by UNIVERSITY OF SOUTHAMPTON HIGHFIELD user on 11 June 2020

Accepted for publication in *Journal of Climate*. DOI10.1175/JCLI-D-19-0083.1.

latitude by 1º longitude, and is equivalent to restoring model salinity to observed in the top 50 m on a timescale of 180 days. Model output is typically stored as annual, monthly and 5-day means. See Madec and the NEMO team (2016) and Aksenov et al. (2016) for further information.

The model circulation in the subpolar North Atlantic was found by Marzocchi et al. (2015) to be consistent with observations and so to be ‘valid and useful’. NEMO exhibits a Labrador Current System in the western Labrador Sea that has a surface signature consistent with satellite altimetry, when viewed both as an annual mean and on shorter timescales (5-day averages; Figure 8 in Marzocchi et al., 2015). NEMO compares favorably with the small number of available observed subsurface velocity sections. For example, the location and speed of the modelled August 2008 Labrador Sea boundary currents were similar to those observed over the same month, and also to a velocity field derived from repeated sections (Hall et al., 2013). The mean total (southward) transport of the model western boundary current was 35-40 Sv, in agreement with sections observed in May 2008 (40 Sv, Hall et al., 2013), August 2014 (42 Sv, Holliday et al., 2018), May 2016 (32 Sv, Holliday et al., 2018) and a mean over 6 sections (33 Sv, Hall et al., 2013).

The Montgomery potential is an exact streamfunction for geostrophic flow on surfaces of constant density anomaly, and it conserves linear potential vorticity along those surfaces. The geostrophic flow can be calculated from the lateral gradient of the Montgomery potential in the same way as it can be found from the lateral gradient of pressure on a constant depth surface. For a Boussinesq model such as NEMO, it is necessary to employ "pseudo-potential density" r_B instead of potential density, and we refer to surfaces of constant r_B as "pseudo-isopycnals". Aksenov et al. (2011) explain the adaptation of the Montgomery potential and its projection on to the model’s pseudo-potential density surfaces. We use model (pseudo-) density surfaces to backtrack flows upstream from the Seal Island measurement location in

Accepted for publication in *Journal of Climate*. DOI10.1175/JCLI-D-19-0083.1.

Downloaded from http://journals.ametsoc.org/jcli/article-pdf/doi/10.1175/JCLI-D-19-0083.1/4954456/jclid190083.pdf by UNIVERSITY OF SOUTHAMPTON HIGHFIELD user on 11 June 2020

order to visualise flow pathways, and we use the Montgomery potential on those surfaces to visualise geostrophic currents.

Freshwater fluxes (F) are calculated from seawater volume transports (V) using the anomaly of salinity with respect to a salinity reference value (S_{REF}), $F = V\,(S - S_{REF})/S_{REF}$. We use S_{REF} = 35.0 for our primary results, which is typical for subarctic regions for the limit of Atlantic-origin waters (e.g. Dickson et al. 1988, 2007; Holliday et al. 2007). Many observation-based studies use a representative Arctic salinity (34.8) as a reference, so we also use the lower value to compare with other studies, as appropriate.

The hydrographic data used to calculate the freshwater content (FWC) of the North Atlantic Ocean is based on the monthly mean objectively-analyzed dataset from the UK Met Office, EN4v2 (Good et al. 2013), accounting for bias using the correction by Gouretski and Resghetti (2010). The data are presented on a grid of 1º latitude x 1º longitude, span 1950-2016, and have been annually averaged before the FWC calculation following the formulation of Boyer et al. (2007) – see their detailed methods:

$$FWC = \int_{z_1}^{z_2} \frac{\rho(T,S,p)}{\rho(T,0,p)} . \frac{S - S_{REF}}{S_{REF}}\, dz$$

where ρ is the sea-water density calculated through the non-linear equation of state (McDougall and Barker, 2011) based on EN4v2 temperature (T) and salinity (S); p denotes pressure that is at the same depth level z, and S_{REF} is the reference salinity as above, 35.0. The depth integration is over the upper 1000 m: specifically between the top 26 depth levels of EN4v2, z_1 = 5 m and z_2 = 968 m of the water column. Grid points with data of fewer than 26 levels (and hence shallower than 968 m) have been masked before calculating FWC.

Downloaded from http://journals.ametsoc.org/jcli/article-pdf/doi/10.1175/JCLI-D-19-0083.1/4954456/jclid190083.pdf by UNIVERSITY OF SOUTHAMPTON HIGHFIELD user on 11 June 2020

Accepted for publication in *Journal of Climate*. DOI10.1175/JCLI-D-19-0083.1.

These have been used to produce annual-mean time series of averaged FWC anomaly relative to climatology (1950-2016) in the North Atlantic.

3. Currents off Labrador

In this section, we aim first (section 3a) to establish the utility of the NEMO model. We describe the model representation of the circulation and properties of the deep ocean and shelf waters of the western Labrador Sea from Davis Strait to Newfoundland, and we compare the model first with published measurements and then with our Seal Island data set. We need the model to represent adequately the regional ocean behaviour so that we can use it (first, section 3b) to test the separability of the constituent parts of the circulation, which requires us to introduce more efficient terminology, and (second, sections 3c,d) to test the following chain of logic. If the annual mean Arctic freshwater export flux through Davis Strait is preserved southwards to Seal Island; if, then, at Seal Island, the annual mean freshwater flux is systematically related to the summertime mean; if, further, a single section measurement is, within uncertainty, representative of the summertime mean; then a Seal Island section measurement may represent the annual mean Arctic freshwater export flux west of Greenland.

We test continuity between Davis Strait and Seal Island for two reasons. The first reason is that Davis Strait is the most convenient location south of the Canadian Arctic Archipelago where all Arctic freshwater exports through the Archipelago are combined. We exclude Fury and Hecla Strait: Tsubouchi et al. (2012) argue that any net throughflow there is very small and much less than measurement uncertainty, as far as can be determined at present. A related reason is that the net freshwater export across the width of Davis Strait, from Baffin Island to Greenland, represents the total Arctic freshwater export through the Archipelago, because there is no northward flow out of the Archipelago into the Arctic. We illustrate this deduction by separating model freshwater fluxes across Davis Strait into three components:

Downloaded from http://journals.ametsoc.org/jcli/article-pdf/doi/10.1175/JCLI-D-19-0083.1/4954456/jclid190083.pdf by UNIVERSITY OF SOUTHAMPTON HIGHFIELD user on 11 June 2020

Accepted for publication in *Journal of Climate*. DOI10.1175/JCLI-D-19-0083.1.

upper-west (the Arctic export flow above 200 m), upper-east (the north-going waters above 200 m), and deep (the net flow below 200 m), where the depth limit approximates the Labrador shelf depth and the horizontal upper division separates the mean locations of south-going and north-going waters (Figure S3). We then calculate annual mean freshwater fluxes in each of the three boxes, plus the total flux across the strait (Figure S4). The upper-west and net freshwater fluxes through Davis Strait (means 128±20 and 109±26 mSv respectively) are correlated r = 0.96, with offset 18±9 mSv (upper-west larger); the other two components are either small (deep segment, 9±1 mSv) or contribute little to the net flux variance (east-upper segment, –27±9 mSv). Since our final results will depend on anomaly fluxes, it makes little difference whether we use Davis Strait net fluxes or those from the upper-west side, which dominates both the magnitude and the variance. Also, ultimately, at Seal Island, we will need to consider the potential separability of the Hudson outflow from the Arctic export flow (sections 3b,e).

a. Comparison of model with measurements

Model mean (1997–2007) surface velocity and salinity, and temperature at 61 m depth (Figure 3) replicate the tripartite structure of the Labrador Current System noted in section 1 above, comprising the recirculating part of the West Greenland Current, the southwards continuation of the Baffin Island Current, and the Hudson Bay outflow (Smith, 1937; Kollmeyer et al., 1967). Much of the West Greenland Current follows the 2000 m isobath, as shown by drifters (Cuny et al. 2002). North of Hudson Strait, the Baffin Island Current lies over the 500 m isobath and follows the same trajectories in the model as measured by floats (LeBlond et al., 1981). Examining the box 66–60 ºW, 60–63 ºN in LeBlond et al. (1981, their Figure 4, our Figure 3), we see (i) the same near-southward pathway around 61 ºW, (ii) the same "C-shaped" diversion towards the mouth of Hudson Strait, and (iii) between 68–65 ºW,

Downloaded from http://journals.ametsoc.org/jcli/article-pdf/doi/10.1175/JCLI-D-19-0083.1/4954456/jclid190083.pdf by UNIVERSITY OF SOUTHAMPTON HIGHFIELD user on 11 June 2020

Accepted for publication in *Journal of Climate*. DOI 10.1175/JCLI-D-19-0083.1.

the same short loop into the mouth of Hudson Strait north of Ungava Bay (Figure 3, Figure S5).

South of Hudson Strait the continuation of the Baffin Island Current joins the recirculating part of the West Greenland Current to form the Labrador Current. Lazier and Wright (1993) estimated that the Labrador Current transported 11.0 Sv southwards off south-east Labrador, based on an August 1988 CTD section initially referenced to a level of no motion at the seafloor on the shelf and at 1500 db on the slope, then adding a barotropic correction mainly derived from year-long current meter records. Despite the significant time difference, our model is consistent with that estimate, giving 11.0 Sv when the same reference levels are used. Transport accumulated from the outer slope to the coast, using the specifications of Lazier and Wright (1993), is in close agreement with their measurements (Figure 4a, and their Figure 7b).

The large catchment area surrounding Hudson Bay supports a fresh outflow to the Labrador Shelf through and on the south side of Hudson Strait, with surface salinities below 30, inshore of the 150 m isobath (Figure 3; Smith et al. 1937; Kollmeyer et al. 1967; Drinkwater 1986). Our model east-going (net) outflow of 1.09 (0.13) Sv for August 2004 to August 2005 agrees with the 1.0-1.2 (~0.1) Sv outflows of Straneo and Saucier (2008) for the same period. Also Drinkwater (1988) find the net outflow to be ~0.1 Sv, using information from a variety of sources. The model net mean (1997-2007) outflow is 0.11 Sv.

We compare the model with Seal Island section measurements during summertime 1995–2010 (Figure 2). In temperature (Figure 2a,e), considering the 0 ºC isotherm, the model CIL is present and has similar lateral extent to the measurements, reaching 170-180 km offshore, while the model CIL is thinner in the vertical than the measurements (~80 m vs. ~120 m respectively). In salinity (Figure 2b,f), model and measurements are very similar: the

Downloaded from http://journals.ametsoc.org/jcli/article-pdf/doi/10.1175/JCLI-D-19-0083.1/4954456/jclid190083.pdf by UNIVERSITY OF SOUTHAMPTON HIGHFIELD user on 11 June 2020

Accepted for publication in *Journal of Climate*. DOI10.1175/JCLI-D-19-0083.1.

shallow isohaline 32.0 is at ~20 m depth in both; the deeper isohaline 34.0 is at 180-200 m depth in both. The fresh coastal wedge of the Hudson Bay outflow is clear, as are the higher offshore salinities of the recirculating West Greenland Current component. Realistic modelled densities (Figure 2c,g) follow from realistic salinities. The two fronts separating the three elements of the current system are seen in the regions of steep density gradient, and result in two surface-intensified velocity jets (Figure 2d,h). Modelled horizontal density gradients are slightly higher than measured so that modelled geostrophic velocities (both referenced to zero at the bottom) are also higher than measured. For instance, the measured peak inshore jet velocity is ~25 cm s^{-1} while the modelled equivalent is ~35 cm s^{-1}. We conclude that the model represents the measured regional features to a sufficiently close approximation, so that we can use the model as required.

b. Sources, pathways and dynamics of the Labrador Current System

We next use the model to track back upstream from the Seal Island section to determine whether the Baffin Island Current, the Hudson Outflow and the recirculating West Greenland Current remain distinct within the Labrador Current System. At this point, we introduce some new water mass terminology. The Arctic-sourced waters of the Labrador Current System that derive from the Baffin Island Current we now call the Arctic Labrador Current water (LC-Arctic), and the part that comprises recirculating Subpolar North Atlantic water from the West Greenland Current we call the Atlantic Labrador Current water (LC-Atlantic).

In the model 1997-2007 mean, the three water masses – Hudson outflow, LC-Arctic and LC-Atlantic waters – are separated at the Seal Island section location by pseudo-isopycnals 25.2 and 26.9 kg m^{-3} (Figure 2e-h). Figure 5 shows two model mean pseudo-isopycnal surfaces, r_B = 25.0 and 26.5 kg m^{-3}; where they exist is coloured, where they do not exist is grey. The two plotted surfaces are close to, but lighter than, the separating densities, so that they

Downloaded from http://journals.ametsoc.org/jcli/article-pdf/doi/10.1175/JCLI-D-19-0083.1/4954456/jclid190083.pdf by UNIVERSITY OF SOUTHAMPTON HIGHFIELD user on 11 June 2020

Accepted for publication in *Journal of Climate*. DOI10.1175/JCLI-D-19-0083.1.

represent the spatial extent of the Hudson outflow (25.0 kg m^{-3}) and LC-Arctic waters (26.5 kg m^{-3}). Plotted on each surface is Montgomery potential and temperature. The Montgomery streamlines (Figure 5a,c) show that the Labrador Current System components follow the same pathways inferred from the surface maps of salinity and velocity (Figure 3). The Baffin Island Current (LC-Arctic) carries Arctic-sourced water (Ingram and Prinsenberg, 1998; Tang et al., 2004), as illustrated by the continuity of the majority of the Montgomery streamlines between Davis Strait and the Labrador shelf (Figure 5c), and by the sub-zero temperatures on r_B = 26.5 kg m^{-3} (Figure 5d). The LC-Arctic water warms on the way south, but remains <0 ºC over most of the Labrador shelf.

The LC-Arctic velocity structure is mainly baroclinic, presenting strong vertical shear with low (<10 cm s^{-1}) bottom velocities, whereas the LC-Atlantic is more barotropic, with higher velocities reaching deeper into the water column and the bottom of the slope (cf. Lazier and Wright 1993). To illustrate this, we calculate the ratio of the bottom velocity to the surface velocity across the model section. Figure 4 shows the absolute velocity at the Seal Island section, the mean offshore limit of the LC-Arctic waters, and the velocity ratio. Across the shelf, this ratio is <25% (more baroclinic), increasing across the shelf slope and through the core of the recirculating Atlantic waters (LC-Atlantic) to ~50% (more barotropic). Figure 2 shows the surface positions of the centres of the model fronts.

We turn next to the presence and influence of the Hudson Bay outflow. The Hudson Bay outflow is represented by the surface r_B = 25.0, where the temperature is ~1 ºC warmer than the LC-Arctic waters (Figure 5a,b). Between the coast and this surface, all the streamlines exit the southern part of Hudson Strait; therefore the waters originate only from Hudson Bay, via the Strait. The streamlines remain tightly constrained to the coast along the Labrador shelf and beyond the Seal Island section, as is also shown by dynamic height derived from early (1928) cross-shelf sections (Smith et al. 1937, their Figure 122). Therefore this is an

Downloaded from http://journals.ametsoc.org/jcli/article-pdf/doi/10.1175/JCLI-D-19-0083.1/4954456/jclid190083.pdf by UNIVERSITY OF SOUTHAMPTON HIGHFIELD user on 11 June 2020

Accepted for publication in *Journal of Climate*. DOI10.1175/JCLI-D-19-0083.1.

inshore jet with behaviour consistent with that of a buoyant coastal current, as noted for the Hudson Strait outflow by Straneo and Saucier (2008), and as seen in comparable systems such as the East Greenland Coastal Current (Bacon et al. 2002, 2014) and the Norwegian Coastal Current (Skagseth et al. 2011). In this case, the excess buoyancy is provided by the freshwater input to Hudson Bay from its surrounding catchment. Scientists familiar with the region call this jet the "inshore branch of the Labrador Current" (e.g. Lazier and Wright 1998, Colbourne 2004). However, we prefer here to recognise that the jet is a geographically and dynamically distinct entity, and we refer to it subsequently as the Labrador Coastal Current (LCC).

To summarise, we decompose the Labrador Current System into three water masses, Hudson outflow, LC-Arctic and LC-Atlantic waters. They meet at two fronts that form the centre of the LCC (Hudson outflow and LC-Arctic waters) and the western edge of the Labrador Current (LC-Arctic and LC-Atlantic waters). Their characteristics remain distinct at the Seal Island section, where the Arctic water fills the shelf between the two fronts, and the CIL lies between the two density surfaces (Figure 2). However, the results to this point do not address the possibility of exchange (i.e. mixing) between the three components of the Labrador Current System, which we consider next.

c. Freshwater transports and continuity

We next compare the NEMO freshwater transports of the Labrador Current System components at the Seal Island section to their source transports, to gain more evidence of their origin, and to quantify how well those source transports are preserved downstream. We examine three locations: the Seal Island transect, the Hudson Strait opening, and Davis Strait (Figure 1).

Downloaded from http://journals.ametsoc.org/jcli/article-pdf/doi/10.1175/JCLI-D-19-0083.1/4954456/jclid190083.pdf by UNIVERSITY OF SOUTHAMPTON HIGHFIELD user on 11 June 2020

Accepted for publication in *Journal of Climate*. DOI10.1175/JCLI-D-19-0083.1.

In Hudson and Davis Straits, net freshwater export is straightforward to compute from the model as coast-to-coast transects, because Hudson Bay is an enclosed basin apart from Fury and Hecla Strait, excluded for the reasons stated above, and because Davis Strait collects all Arctic outflows through the Canadian Arctic Archipelago, where there is no northward / poleward imports from the south, through the Archipelago and into the high Arctic Ocean: the West Greenland Current recirculates within Baffin Bay and the small southern basins of Nares Strait. The Seal Island section terminates in the open ocean, so we distinguish between the Hudson outflow, LC-Arctic, and LC-Atlantic waters as follows. The delimiting pseudo-isopycnals vary with time, so they are computed for each model time step. For the coastal front where the Hudson outflow and LC-Arctic waters meet, we find the location of maximum surface velocity. For the shelf edge front, where the LC-Arctic and LC-Atlantic waters meet, we find the maximum near-surface density gradient at the shelf edge; velocity is not unambiguous, because the LC-Atlantic (further offshore) presents lower density gradients but higher velocities. Therefore we select the frontal density at 25 m depth, below the seasonal thermocline, to avoid bias from summer surface warming; see Figure 2. Figure 6 shows the model monthly and annual mean freshwater transports between 1995–2010 as time series and seasonal cycles, to compare (i) the Hudson outflow at Seal Island and the Hudson Strait exit, and (ii) the LC-Arctic water at Seal Island and at Davis Strait. Annual means at Davis Strait are calculated January–December, and at Seal Island, with a 2-month lag, March–February.

The long-term model mean (1995-2010) freshwater transports at the Seal Island section of the Hudson outflow (45 mSv) and LC-Arctic (112 mSv) waters agree with their respective sources, the Hudson Strait outflow (43 mSv) and the Davis Strait transport (109 mSv), and they also agree reasonably with the 41 and 130 mSv calculated by Mertz et al. (1993), who use the same data as Lazier and Wright (1993). Comparison of the model annual mean

Downloaded from http://journals.ametsoc.org/jcli/article-pdf/doi/10.1175/JCLI-D-19-0083.1/4954456/jclid190083.pdf by UNIVERSITY OF SOUTHAMPTON HIGHFIELD user on 11 June 2020

Accepted for publication in *Journal of Climate*. DOI10.1175/JCLI-D-19-0083.1.

freshwater fluxes at Davis Strait and Seal Island (Figure 6) provides further evidence of continuity (Figure S6). The correlation between the two time series is very high (r = 0.95). As a point of interest, we observe that modelled freshwater fluxes at Seal Island are highly-dependent on seawater volume transport (and therefore velocity), while there is no systematic dependence on salinity (Figure S7).

Two other subsidiary sources of freshwater are quantified as follows. First, surface freshwater flux resulting from model surface salinity relaxation. The shelf between Hudson Strait and Seal Island has length ca. 800 km and width ca. 150 km, for area 1.2 x 10^{11} m^2; the surface mass flux over the shelf due to salinity restoration is ca. 3 x 10^{-5} kg m^{-2} s^{-1} (not shown), for a total mass flux of 4 x 10^6 kg s^{-1}, equivalent to a freshwater volume flux (out of the ocean) of 4 mSv. Second, surface freshwater flux resulting from the net of precipitation over evaporation (net P–E). With the same shelf area and annual net P–E of 1 m yr^{-1} (e.g. Josey & Marsh 2005), equivalent to 3 x 10^{-8} m s^{-1}, for a net freshwater flux (into the ocean) over the shelf of 4 mSv. These subsidiary sources are negligible.

Howatt et al. (2018) analyse Ekman and eddy exchange of freshwater across the Labrador shelf break. Working a little south of Seal Island, they diagnose the freshwater transport from the shelf to the deep basins as just a few mSv. As part of their analysis, they estimate the corresponding upper-ocean horizontal diffusivity as $k_h \sim 100$ m^2/s. With a shelf width W ~200 km, the approximate timescale for eddies to transport water across the width of the shelf is $W^2/k_h = 4 \times 10^8$ s, or >10 years. The transit time down the shelf between Davis Strait, Hudson Strait and Seal Island is a few months, so that there is little impact on freshwater fluxes on the shelf by exchanges between on-shelf and deeper waters.

Downloaded from http://journals.ametsoc.org/jcli/article-pdf/doi/10.1175/JCLI-D-19-0083.1/4954456/jclid190083.pdf by UNIVERSITY OF SOUTHAMPTON HIGHFIELD user on 11 June 2020

Accepted for publication in *Journal of Climate*. DOI10.1175/JCLI-D-19-0083.1.

This evidence of continuity means that there is no significant loss offshore of on-shelf freshwater, nor is the on-shelf freshwater flux significantly impacted by on-shelf transport of offshore saline waters.

Benetti et al. (2017) show that the coastal wedge of freshwater (the Hudson outflow) contains the signature of meteoric water (precipitation and riverine inputs) that is not present elsewhere on the shelf, and which is found, from physical and geochemical characteristics, to originate mainly from Hudson Bay. They also conclude that the mid-shelf water (our LC-Arctic water) is of Arctic origin, having passed through Davis Strait, in contrast to the West Greenland Current-sourced water (our LC-Atlantic) over the slope and the outer shelf. This is consistent with our results.

We conclude that both freshwater export fluxes – the Arctic flux from Davis Strait and the Hudson outflow – can be calculated at the Seal Island section.

d. Summertime representativeness

We have determined (section 3 above) that freshwater fluxes are preserved between the choke points of Davis and Hudson Straits and the Seal Island section measurement location. We now wish to determine from the model the extent to which single, summertime section occupations may be representative of longer-term variability. We assume that a model 5-day mean is representative of a typical expedition timescale, and that we can then estimate the uncertainty inherent in a single section measurement by calculating the uncertainty of all 5-day means within a specified "summertime" period.

We consider here the Arctic (LC-Arctic) freshwater flux; consideration of the Hudson outflow will follow in section 4. We inspect the 1/12º NEMO model by comparing the annual mean (January-December) freshwater fluxes with the summertime (July-August) mean

Accepted for publication in *Journal of Climate*. DOI10.1175/JCLI-D-19-0083.1.

Downloaded from http://journals.ametsoc.org/jcli/article-pdf/doi/10.1175/JCLI-D-19-0083.1/4954456/jclid190083.pdf by UNIVERSITY OF SOUTHAMPTON HIGHFIELD user on 11 June 2020

(Figure S8). The summertime mean was constructed from 12 sequential 5-day means spanning July-August. The start month for the annual means (January) was chosen as showing the highest correlation (r=0.89) between summertime and all 12 possible versions of annual means. Mean summertime freshwater fluxes (99 mSv) are weaker than mean annual fluxes (116 mSv); the offset is 17 ±14 mSv (1 sd), likely reflecting seasonal variability in sea ice export and wind velocity.

To assess the representativeness of the two-month summertime means in comparison with typical section measurement durations, we next inspect the variability of model 5-day mean freshwater fluxes within the summertime means. For the 1/12^{o} model, the summertime standard deviation is 17 mSv, for a total (root-sum-square) uncertainty, including the summer-to-annual offset, of 22 mSv. This quantification of mean offset and uncertainty between freshwater fluxes calculated on a summertime "expedition" timescale (the model 5-day mean) and the annual mean will be used in the measurement context in the next section.

4. Seal Island freshwater fluxes

In this section, we first calculate freshwater fluxes from the Seal Island section measurements separately for Hudson outflow and LC-Arctic waters. Then we compare these fluxes with other metrics – both to explore the implications of the new information, and also as a consistency check, to confront our new freshwater flux estimates with related but independent quantities. For context, we provide in Table 1 summertime (1995-2010) seawater transport statistics for measurements and models and for both Hudson outflow and LC-Arctic waters, showing that the mean transport for the Hudson outflow is ~0.3±0.1 Sv and for the LC-Arctic waters is ~1.1±0.3 Sv. There is a strong implication that the (constant) transport offset provided by the NEMO bottom velocities is an over-estimate; however, it does not affect our assessment of variability.

Downloaded from http://journals.ametsoc.org/jcli/article-pdf/doi/10.1175/JCLI-D-19-0083.1/4954456/jclid190083.pdf by UNIVERSITY OF SOUTHAMPTON HIGHFIELD user on 11 June 2020

Accepted for publication in *Journal of Climate*. DOI 10.1175/JCLI-D-19-0083.1.

a. Seal Island freshwater flux calculation

In section 3, we showed (i) that freshwater fluxes from the Davis and Hudson Straits were adequately preserved at the Seal Island section location, and (ii) that section occupations are representative of the year in which they were made. We now turn to the Seal Island section measurements, and describe how we calculate the Hudson outflow and LC-Arctic freshwater flux time series.

To identify two density surfaces to separate the two export fluxes, we approach the measurement calculation differently from the model, because we lack measurements of absolute velocity, and because the measurements' horizontal resolution is generally lower than the models'. We revert to the original definitions of the temperature-delimited CIL, and apply those limits (–1, 0, 1 ºC) in temperature-salinity (θ-S) phase space. Figure S9 shows θ-S diagrams for the whole data set and for each decade. For each occupation of the section, we obtain maximum and minimum densities at each CIL limit temperature, separating Hudson outflow and LC-Arctic from LC-Atlantic waters. The resulting density surfaces are illustrated in Figure 2. We calculate geostrophic velocities referenced to zero velocity at the bottom. For scaling and illustration, we then add a barotropic velocity correction using the NEMO 1/12º summertime (July-August) 1995-2010 mean of the bottom velocity at each station pair location (see Figure 4). These barotropic velocities are fixed: we do not attempt to include model temporal variability. However, the freshwater flux uncertainties that result from their variability are low, at 1-2 mSv (1 sd). They add 24 mSv to the Hudson outflow and 54 mSv to the LC-Arctic freshwater fluxes.

b. Labrador Coastal Current and Hudson Bay

If Hudson Bay only received freshwater from runoff, it would be a freshwater lake. It is saline because it also receives seawater from the Arctic. So, before turning to Hudson

Downloaded from http://journals.ametsoc.org/jcli/article-pdf/doi/10.1175/JCLI-D-19-0083.1/4954456/jclid190083.pdf by UNIVERSITY OF SOUTHAMPTON HIGHFIELD user on 11 June 2020

Accepted for publication in *Journal of Climate*. DOI10.1175/JCLI-D-19-0083.1.

outflow freshwater fluxes, we examine Hudson Strait and Bay (excluding Fury and Hecla Strait; section 3). The Hudson Bay salinity import arises from the part of the Davis Strait export that enters via the north side of Hudson Strait from the east; cf. Figure 5c, nearshore streamlines on $r_B = 26.5$ kg m^{-3}. We now examine the impact of this 'diversion' of Arctic freshwater exports, because it must eventually emerge again in the Hudson outflow.

The 1/12º NEMO model shows that Hudson Strait supports bi-directional flow, with the north side westward, supplied by the Davis Strait outflow, and south side eastward, forming the Hudson outflow (figure S5, Figure 5), which is possible because the deformation radius of 5-7 km (Nurser and Bacon 2014) is much lower than the strait width, *ca.* 100 km. The apparent magnitude of the countervailing transports reduces westwards, from *ca.* 0.5 Sv (east end) to 0.2 Sv (west end) through cross-strait exchanges modulated by recirculations. Relevant timescales will therefore vary widely: for Hudson Bay, with volume ~10^{14} m^3 (Jakobsson 2002) and seawater import 0.5 (0.2) Sv, the mean residence time is ~7 (25) years; for the short "loop" from the Strait's eastern entrance to north of Ungava Bay, the advection timescale is a few months. Nevertheless, we can simply estimate the freshwater 'diversion' rate. The Davis Strait salinity near the west side is ~32.5 (Curry et al. 2014), so with S_{REF} = 35.0 and mean seawater flux 0.5 (0.2) Sv, the associated freshwater flux is ~35 (14) mSv. Given the range of time lags between entry and exit, we do not attempt further refinement, but treat this as an offset included in the Hudson outflow as part of the Arctic freshwater export flux.

Turning now to the Hudson outflow, we have its freshwater flux time series (Figure 7a), calculated as in section 3. We expect its freshwater burden mainly to comprise (i) the 'diversion' flux described above, and (ii) river and other terrestrial runoff from the Hudson Bay catchment and the coast up to the Seal Island section. We note first the similarity between the early 1990s Hudson outflow freshwater flux minimum and a parallel minimum in

Downloaded from http://journals.ametsoc.org/jcli/article-pdf/doi/10.1175/JCLI-D-19-0083.1/4954456/jclid190083.pdf by UNIVERSITY OF SOUTHAMPTON HIGHFIELD user on 11 June 2020

Accepted for publication in *Journal of Climate*. DOI10.1175/JCLI-D-19-0083.1.

Hudson Bay runoff (Déry et al. 2005, their Figure 6), so we compare the Hudson outflow time series at Seal Island with the multi-decadal time series of annual mean regional runoff volumes (Déry et al. 2016). Dividing the catchment into four regions – the Labrador Coast, Hudson Strait (including Ungava Bay), and eastern and western Hudson (including James) Bay (see Déry et al. 2016, their Figure 1) – their mean annual river runoff rates were (respectively) 77, 114, 202 and 323 km^3/yr, for a total ~700 km^3/yr, or ~25 mSv. We expected to see reducing (lagged) correlations between the two with increasing distance from Seal Island, which is what we find: maximum correlations (with lag) between the four regions and the Seal Island Hudson outflow were (respectively) r = 0.45 (1 yr), 0.45 (2 yr), 0.14 (3 yr), 0.29 (3 yr). The four regional runoff fluxes are summed using those lags and shown in Figure 7b; the overall correlation between this new runoff total and the Hudson outflow is r = 0.48 (see also Figure S10). There is an interesting preservation of the river runoff signal out of Hudson Bay and down the Labrador coast, therefore, with the magnitude of the runoff signal mainly determined by the two largest sources, and the variability mainly determined by the two smallest ones – and those smallest ones are closest to the Seal Island section.

The mean Hudson outflow and runoff freshwater fluxes are 57 and 23 mSv respectively (Figure 7), and the difference between them 34 mSv, nearly the same as the 35 mSv 'diversion' flux obtained above. Using the linear regression of Hudson outflow on total runoff freshwater fluxes, we also find that for zero runoff, the Hudson outflow freshwater flux is 47 mSv, which is an independent estimate of the 'diversion' flux, but is more uncertain. A more sophisticated analysis would include runoff seasonality and Hudson Bay and Strait dynamics and timescales, but this is beyond the present scope.

We also speculate on the nature of the warm and fresh summertime "cap" over the CIL. Myers et al. (1990) attribute it to summertime sea ice melt, but there could also be a contribution from seasonal relaxation (horizontal "slumping") of the LCC isopycnals, causing

Accepted for publication in *Journal of Climate*. DOI10.1175/JCLI-D-19-0083.1.

Downloaded from http://journals.ametsoc.org/jcli/article-pdf/doi/10.1175/JCLI-D-19-0083.1/4954456/jclid190083.pdf by UNIVERSITY OF SOUTHAMPTON HIGHFIELD user on 11 June 2020

Hudson outflow waters to spread offshore, as seen in the East Greenland Coastal Current (Bacon et al. 2014).

c. Arctic freshwater exports (LC-Arctic waters)

The LC-Arctic freshwater flux time series for 1950–2016, using the 0 ºC definition of the CIL, is shown in Figure 8a, and its uncertainty resulting from use of the three CIL definitions is shown as anomalies about the record means in Figure 8b. The average LC-Arctic freshwater transports for the whole time series (1950-2016) for CIL definitions –1, 0 and 1 ºC are 99, 137 and 162 mSv (respectively), which all include 54 mSv from the (constant) barotropic offset (section 4a), but do not include either the summer-to-annual offset of ca. 22 mSv (section 3d) or the 'diversion' flux of 35 mSv (section 4b); therefore the long-term annual mean could be as high as 194 mSv (for the 0 ºC version). The different CIL-derived definitions have little impact on the anomaly timeseries (Figure 8b) because the lower-density surface (depths shallower than ~50 m) occurs where the stratification is stronger and velocities higher, so its depth varies little, while the depth range of the higher-density surface is expanded by ~100 m, but both stratification and velocities are weaker there (Figure 2). The resulting uncertainty is 8 mSv (1 sd).

The equivalent quantity to LC-Arctic water in Curry et al. (2014) is their Arctic Water, defined with temperature <2 ºC and salinity <33.7, measured between October 2004 and September 2010, and they plot its freshwater transport by month (their figure 9), but do not calculate its mean, which we estimate to be ~90-100 mSv, and to which we add their sea ice transport of 10 mSv, for total of 100-110 mSv. Our estimate for the same period and S_{REF} = 34.8 is 68 mSv (76 mSv, S_{REF} = 35.0); adding 57 mSv for the two offsets (as above) brings our total to 125 mSv, in reasonable agreement with Curry et al. (2014); but this does indicate

Accepted for publication in *Journal of Climate*. DOI10.1175/JCLI-D-19-0083.1.

Downloaded from http://journals.ametsoc.org/jcli/article-pdf/doi/10.1175/JCLI-D-19-0083.1/4954456/jclid190083.pdf by UNIVERSITY OF SOUTHAMPTON HIGHFIELD user on 11 June 2020

that our analysis is robust, given that none of the three offsets (barotropic, summer-to-annual and 'diversion') contains variability.

We cannot be certain that the apparent interannual variability in the LC-Arctic freshwater flux (Figure 8) is real, given the pointwise uncertainty of ~20 mSv (section 3d), our lack of knowledge of the 'diversion' uncertainty, and the very low apparent uncertainty of the barotropic offset. However, one individual instance is probably real: the very high freshwater flux in 1972 (226 mSv), which resulted from an unprecedented quantity of very cold intermediate water (Templeman 1975), later interpreted as the Great Salinity Anomaly reaching the region (Dickson et al. 1988). However, clear long-term (multi-annual to decadal) variability, amplitude ~30 mSv, emerges from the smoothed time series (Figure 8, 7-year running mean), with high freshwater transports during the 1950s and 1970s–80s, and low transports in the 1960s, and from the mid-1990s to the present, reflected in the decadal-scale expansion and contraction of the CIL (Figure S2). If we assume (conservatively) the total uncertainty of the barotropic and 'diversion' fluxes to be 50% of the mean (57 mSv), therefore 29 mSv, and we add that (root-sum-square) to the ~20 mSv pointwise uncertainty, the total is 35 mSv, and its filtered standard error (n=7) is then 13 mSv; then the long-term variability is likely real. We see then that the Curry et al. (2014) 2005-10 measurements were made during a sustained period of low freshwater export. They also calculate freshwater fluxes for (geographically more limited) measurements made in Davis Strait 1987-90, and find significantly higher values – by ~40% – for which our new results provide clear context and support.

We have addressed above the various offsets that contribute to the total freshwater flux in order to identify and quantify the main processes that contribute to the total. Various approaches to determining the net Arctic surface freshwater flux have settled on a mean value of order 200 mSv, whether from data compendia (Haine et al. 2015), high-resolution ice-

Downloaded from http://journals.ametsoc.org/jcli/article-pdf/doi/10.1175/JCLI-D-19-0083.1/4954456/jclid190083.pdf by UNIVERSITY OF SOUTHAMPTON HIGHFIELD user on 11 June 2020

Accepted for publication in *Journal of Climate*. DOI 10.1175/JCLI-D-19-0083.1.

ocean models (Bacon et al. 2015), or an annual mean derived from monthly synoptic measurements (Tsubouchi et al. 2018). Given that we expect (approximately) half that total to emerge through Fram Strait (de Steur et al. 2009, Spreen et al. 2009), our model-derived freshwater flux offsets must be quantitatively suspect (i.e over-estimates), but with the lack of long-term measurements of absolute velocities at the Seal Island section, we recognise that we cannot yet substantively address their variability.

However, the flux anomalies (Figure 8b) are derived purely from measurements and are a quantitative reflection of Arctic freshwater export variability west of Greenland, so we next compare the three versions (based on –1, 0 1 ºC CIL definitions) of the anomaly fluxes and confront them, and their cumulative freshwater volumes, with long-term freshwater storage measurements in the Arctic and Subpolar North Atlantic Oceans (Figure 9). We note first that there is little difference between the cumulative freshwater volumes derived from the 0 and 1 ºC CIL definitions but that the –1 ºC version is biased high. In all three cases, the lower the defining temperature, the lower the enclosed area and the lower the seawater and freshwater transports but the higher their variability as the shape enclosed becomes more complex (e.g. Figure S2).

We now compare Arctic freshwater storage changes (Polyakov et al. 2013) to the (smoothed) Seal Island Arctic freshwater transports (Figure 9). Long periods of high freshwater transport precede long periods of low freshwater storage, with the highest correlation ($r = -0.73$) at 6-7 years lag. Cumulative Seal Island freshwater volumes (Figures 9 and S11) are weakly correlated ($r = -0.35$) with, and precede, the same Arctic freshwater storage changes, at 7-8 years lag. A consistent interpretation (phrased colloquially) is that when atmospheric dynamics 'open the gates', seawater is released from the Arctic, likely via both routes (west and east of Greenland), but it takes some time (~7 years) for the drawdown to impact on Arctic freshwater storage – meaning to travel from the source region (the Beaufort Gyre) to

Downloaded from http://journals.ametsoc.org/jcli/article-pdf/doi/10.1175/JCLI-D-19-0083.1/4954456/jclid190083.pdf by UNIVERSITY OF SOUTHAMPTON HIGHFIELD user on 11 June 2020

Accepted for publication in *Journal of Climate*. DOI10.1175/JCLI-D-19-0083.1.

the Atlantic and Nordic Seas. The 'choice' of two routes means that while rates from the western route correlate well with storage, the allied volumes correlate less well. This may be consistent with the analysis of Lique et al. (2009); testing of this supposition urgently requires a long and consistent time series of solid and liquid freshwater exports from Fram Strait.

Accumulating the Seal Island freshwater export anomaly generates a time series of cumulative freshwater volume that agrees closely with North Atlantic freshwater storage in both amplitude and phase (Figure S11); see Peterson et al. (2006), whose domain comprises the Nordic Seas, the subpolar North Atlantic and the subtropical North Atlantic deeper than 1500 m. This is surprising, given the expected (if unquantified) contribution to total freshwater export variability from Fram Strait. We note that Fram Strait lies some distance from the North Atlantic proper, with the Nordic Seas buffering the freshwater export. Between Fram and Denmark Straits, the Jan Mayen and East Iceland Currents (e.g Rudels et al. 2002, Macrander et al. 2014) remove portions of the East Greenland Current which then recirculate within the Nordic Seas. Then the source variability of their freshwater transports may be obscured by surface buoyancy fluxes and by horizontal and vertical mixing imposed on long timescales, perhaps resulting in local, shorter-term variability dominating eventual freshwater export from the Nordic Seas into the North Atlantic. This raises questions about the role of other contributions to the regional freshwater content variability, including surface fluxes and ocean sources from the south.

Pursuing this line of enquiry further, we investigate a simpler metric than that of Peterson et al. (2006) by inspecting changes in freshwater content in the Subpolar North Atlantic (Figure 9), which show surprisingly high correlation with our Arctic freshwater export flux anomalies ($r = 0.81$ at 2 years' lag). Correlation is not causation, however. Differentiating (with respect to time) the sub-polar North Atlantic freshwater content anomalies, to generate an annual time

Downloaded from http://journals.ametsoc.org/jcli/article-pdf/doi/10.1175/JCLI-D-19-0083.1/4954456/jclid190083.pdf by UNIVERSITY OF SOUTHAMPTON HIGHFIELD user on 11 June 2020

Accepted for publication in *Journal of Climate*. DOI10.1175/JCLI-D-19-0083.1.

series of equivalent freshwater fluxes, produces a standard deviation of 52 mSv, which is nearly double our observed Arctic freshwater export value. This raises two possible approaches to explanation: that other freshwater flux inputs to and outputs from the sub-polar North Atlantic are (1) "flat" (i.e. invariant, or otherwise weakly varying), so that they are largely absent when considering anomalies; and / or (2) also correlated in a similar manner, so that they reinforce the changes brought about by the Seal Island Arctic freshwater transport, to generate the observed sub-polar North Atlantic freshwater content variability. Evidence to support the second option is given by Boyer et al. (2007), who show the variability (annual, 1955-2005; their figure 5) in the anomaly of precipitation minus evaporation (P–E) over the sub-polar North Atlantic, with a range of ±3000 km^3, and a positive correlation (r = 0.68) with regional freshwater content. These correlations implicate large-scale (Arctic / North Atlantic) atmospheric as well as oceanic processes, but again, more research is needed.

5. Conclusions and future prospects

We have used a 7-decade-long time series of hydrographic observations on the Labrador shelf to generate a new, annually-resolved record of ocean freshwater transports, and particularly transport anomalies, west of Greenland. With support from high-resolution model runs, we identify the three components of the Labrador Current System, so that we can first exclude the offshore, recirculating component from the North Atlantic Subpolar Gyre. We then inspect the Labrador Coastal Current and demonstrate the Hudson outflow waters' direct link to Hudson Bay river runoff. Finally we isolate the central component and show that it is (much of) the Arctic freshwater export west of Greenland, with the remainder experiencing diversion via Hudson Bay. The new time series of Arctic freshwater transports shows high export rates during the 1950s and 1970s–80s, and low rates in the 1960s, and from the mid-1990s to 2016.

This record correlates interestingly with records of freshwater storage of similar duration for

Downloaded from http://journals.ametsoc.org/jcli/article-pdf/doi/10.1175/JCLI-D-19-0083.1/4954456/jclid190083.pdf by UNIVERSITY OF SOUTHAMPTON HIGHFIELD user on 11 June 2020

Accepted for publication in *Journal of Climate*. DOI10.1175/JCLI-D-19-0083.1.

the Arctic and North Atlantic Oceans, which supports, qualitatively and quantitatively, the realism of our new record.

Our results also point towards further research requirements. First, it is clear that generation of a long and consistent record of solid and liquid freshwater fluxes in both Fram and Davis Straits is urgently needed, so that we may better understand what controls relative variability in the two Arctic Ocean freshwater export routes east and west of Greenland. Second, better understanding is needed of the physical mechanisms that not only govern storage and release of freshwater within the Arctic, but also control the promotion and restraint of the transfer of freshwater from the Arctic Ocean to the receiving basins (the North Atlantic and Nordic Seas), and further (perhaps), the buffering of the freshwater export variability, particularly by the Nordic Seas. Third, we infer an atmospheric connection between Arctic Ocean freshwater storage and North Atlantic P–E, which is obscure to us at present, but given the large regional scale of coherent patterns of atmospheric variability such as the Arctic Oscillation (Thompson and Wallace 1998), not implausible. Fourth, better appreciation of circulation, storage and timescales in Hudson Bay would likely improve the link between the catchment runoff and its manifestation as part of the LCC along the Labrador shelf (cf. Ridenour et al. 2019); the potential exists for the Hudson outflow to act as a "continent-scale rain gauge".

Fifth, there is the evident importance of the absolute circulation on the Labrador shelf. It supports about half of the total Arctic freshwater export into the North Atlantic as well as the runoff from the Hudson Bay catchment. To simplify the problem and for consistency, we have concentrated on Seal Island summertime measurements, but there remains an unexploited archive of hydrographic measurements on the Seal Island section and elsewhere on the east Canadian shelf covering many years and made at different times of year, which would help to elucidate the seasonal cycle. We urgently require better knowledge and understanding of absolute seawater and freshwater transports and of local and remote

Downloaded from http://journals.ametsoc.org/jcli/article-pdf/doi/10.1175/JCLI-D-19-0083.1/4954456/jclid190083.pdf by UNIVERSITY OF SOUTHAMPTON HIGHFIELD user on 11 June 2020

Accepted for publication in *Journal of Climate*. DOI 10.1175/JCLI-D-19-0083.1.

mechanisms controlling their variability here, which would likely increase the accuracy (reduce the uncertainty) of our freshwater transport records. This would also be of use to the Overturning in the Subpolar North Atlantic Program (OSNAP; Lozier et al. 2017, 2019), which aims to monitor the mass, heat and freshwater fluxes between Greenland, Canada and Scotland. Its western terminus is at *ca.* 53 ºN, comprising deep-water and shelf-break moorings that do not extend across the shelf. We only presently have snapshots of the absolute shelf circulation (e.g Holliday et al. 2018), so the first requirement here is direct (measured) knowledge of the ice and ocean seasonal cycle in terms of (spatially-resolved) currents, salinities and temperatures. Ideally, technology will permit continuous monitoring of the on-shelf property transports in this difficult location.

To conclude, we offer some thoughts about our (conventional) approach to freshwater flux calculation. Bacon et al. (2015) develop a new freshwater flux framework starting from the perception that the only unique and non-arbitrary ocean freshwater flux is the surface flux (P–E plus runoff). Using the control volume approach and allowing variability in surface freshwater fluxes and in (ice and ocean) boundary fluxes and storage of mass and salinity, a surface freshwater flux expression results that is similar to the conventional oceanic one (as in section 2), but with the reference salinity replaced by the ice and ocean mean salinity around the ocean boundary of the control volume. This has the uncomfortable consequence that the boundary mean salinity can vary with time. However, it also allows for unambiguous interpretation: the surface freshwater flux (in the Arctic case) dilutes the ocean inflows to become the outflows. A further refinement is given in Carmack et al. (2016, Appendix A): the surface freshwater flux combines with the low salinity of the Bering Strait inflow to the Arctic to dilute the inflowing Atlantic-origin waters to become the outflows. This is relevant to the present Labrador case because the control volume can be defined as the ocean within (poleward of) the boundary of the OSNAP section (Canada to Greenland to Scotland) plus

Downloaded from http://journals.ametsoc.org/jcli/article-pdf/doi/10.1175/JCLI-D-19-0083.1/4954456/jclid190083.pdf by UNIVERSITY OF SOUTHAMPTON HIGHFIELD user on 11 June 2020

Accepted for publication in *Journal of Climate*. DOI10.1175/JCLI-D-19-0083.1.

Bering Strait, for which the boundary mean salinity is ~35 – hence our choice of reference salinity. However, Schauer and Losch (2019), entitled "freshwater in the ocean is not a useful parameter in climate research", offer a radically different view: noting that freshwater fractions are arbitrary, they recommend using instead the salinity budget. Both of these approaches are demonstrably true and ought, therefore, to be compatible. The old subjects of ocean freshwater fluxes and/or salinity fluxes still require development.

Downloaded from http://journals.ametsoc.org/jcli/article-pdf/doi/10.1175/JCLI-D-19-0083.1/4954456/jclid190083.pdf by UNIVERSITY OF SOUTHAMPTON HIGHFIELD user on 11 June 2020

Accepted for publication in *Journal of Climate*. DOI10.1175/JCLI-D-19-0083.1.

Acknowledgments. CFL received funding from University of Southampton, Obra Social La Caixa and NOC during his PhD. We thank Stephen Déry for providing the Canadian runoff data, and Hydro Québec for allowing use of proprietary data. This is a contribution to: NERC National Capability via the Atlantic Climate System Integrated Study; the Overturning in the Subpolar North Atlantic Program (OSNAP, NERC NE/K010875/1); and The Environment of the Arctic – Climate, Ocean and Sea Ice (TEA-COSI, NERC NE/I028947/1). LC acknowledges support through the Swedish National Space Board (SNSB; Dnr. 133/17). Data access is as follows: the Seal Island section, part of the Fisheries and Oceans Canada Atlantic Zone Monitoring Program, www.meds-sdmm.dfo-mpo.gc.ca; ETOPO2v2, www.ngdc.noaa.gov/mgg/global/etopo2.html; the General Bathymetric Chart of the Oceans (GEBCO), www.gebco.net; and EN4, https://www.metoffice.gov.uk/hadobs/en4/.

Downloaded from http://journals.ametsoc.org/jcli/article-pdf/doi/10.1175/JCLI-D-19-0083.1/4954456/jclid190083.pdf by UNIVERSITY OF SOUTHAMPTON HIGHFIELD user on 11 June 2020

Accepted for publication in *Journal of Climate*. DOI10.1175/JCLI-D-19-0083.1.

Appendix A: Seal Island Section data characteristics and quality control.

The earliest measurements (accuracy) used bottles with reversing thermometers (0.02 ºC); electronic bathythermographs were introduced in the 1960s (0.2 ºC), and CTDs in the late 1970s (0.005 ºC). Salinity accuracy improved from 0.02 for bottle titrations to 0.005 for CTD measurements (Colbourne et al. 1995). Standard station positions are listed in Table A1.

The total number of available profiles was 3905, beginning 1928. All calendar months have been measured at some time, but the observations are heavily weighted towards summer (meaning July and August) and November, and of these, summer provides the longer time series, consistent from 1950 to present, and the higher data density. Quality control is required to identify usable sections, and the steps in the process follow. The number of stations remaining after each step is given in braces.

1. Season: select summer data only {1649}.

2. Time range: 1950 to present, because this period provides over 6 decades of continuous data {1583}. This is also when conductivity replaced titration for salinity measurement (Thomson and Emery 2014).

3. Exclude profiles lacking salinity {1135}.

4. Vertical resolution: a minimum of 4 depth points per profile is set {1110}.

5. Proximity to the standard section location: maximum deviation of station position from the standard section is set to 15 km, except for 3 years with high station density (1985, 1987 and 1988), when it is set to 5 km {857}.

6. Removal of depth-binned profiles and replacing with original data {813}.

Downloaded from http://journals.ametsoc.org/jcli/article-pdf/doi/10.1175/JCLI-D-19-0083.1/4954456/jclid190083.pdf by UNIVERSITY OF SOUTHAMPTON HIGHFIELD user on 11 June 2020

Accepted for publication in *Journal of Climate*. DOI10.1175/JCLI-D-19-0083.1.

7. Removal of duplicate records (2 types): (i) duplicate files with the same information, and (ii) quasi-simultaneous profiles that are either immediately repeated casts or a station sampled with two different instruments, where there were 6 profile pairs, and the profile to use was selected for consistency with adjacent stations {760}.

8. Synopticity: most sections take a week to complete, and the standard section is often measured in under 5 days, yet some years present profiles over a month apart. To remove instances of temporal discontinuity, we find the observation median time and disregard profiles outside ±10 days of that time {726}.

9. Proximity: some profile pairs lie too close to each other, so we set a minimum station separation of 3 km, and consider any nearly overlying profile as a repeated station (cf. step 7). This allows for moderate ship drift and is less than the shortest distance between standard stations (15 km), so that section resolution may be improved with intermediate stations {679}.

10. Section coverage: we reject occupations of the Seal Island section with inadequate coverage, meaning those with <6 stations, and those missing the inshore and offshore ends of the section {664}.

11. Final visual inspection: six stations were rejected. Cases included mis-recording of date, bad station positions, and incomplete profiles {658}.

To grid the sections, we first project the stations orthogonally onto the Seal Island standard line, with coordinates computed as *latitude* = 0.5818 × *longitude* + 85.6152, the best fit to standard station positions. Pressure is converted to depth using Fofonoff and Millard (1983), and binned to 1 m depth intervals. Profiles are then gridded using linear interpolation with 2.5 km horizontal resolution, ensuring that no two stations are averaged together, and yielding

Downloaded from http://journals.ametsoc.org/jcli/article-pdf/doi/10.1175/JCLI-D-19-0083.1/4954456/jclid190083.pdf by UNIVERSITY OF SOUTHAMPTON HIGHFIELD user on 11 June 2020

Accepted for publication in *Journal of Climate*. DOI10.1175/JCLI-D-19-0083.1.

at least 5 intermediate points between the two closest standard stations. This procedure generates summer sections of T, S and density for 60 of the 67 years between 1950–2016.

Downloaded from http://journals.ametsoc.org/jcli/article-pdf/doi/10.1175/JCLI-D-19-0083.1/4954456/jclid190083.pdf by UNIVERSITY OF SOUTHAMPTON HIGHFIELD user on 11 June 2020

Accepted for publication in *Journal of Climate*. DOI10.1175/JCLI-D-19-0083.1.

References

Aksenov, Y., S. Bacon, A. C. Coward, and N. P. Holliday, 2010: Polar outflow from the Arctic Ocean: a high resolution model study. *J. Mar. Syst.*, **83**, 14–37, https://doi.org/10.1016/j.jmarsys.2010.06.007.

Aksenov, Y., V. V. Ivanov, A. Nurser, S. Bacon, I. V. Polyakov, A. C. Coward, A. C. Naveira- Garabato, and A. Beszczynska-Moeller, 2011: The Arctic circumpolar boundary current. *J. Geophys. Res.*, **116**, C09017, https://doi.org/10.1029/2010JC006637.

Aksenov, Y., and Coauthors, 2016: Arctic pathways of Pacific water: Arctic Ocean model intercomparison experiments. *J. Geophys. Res.*, **121**, 27–59, https://doi.org/10.1002/2015JC011299.

Armitage, T. W. K., S. Bacon, A. L. Ridout, S. F. Thomas, Y. Aksenov, and D. J. Wingham, 2016: Arctic sea surface height variability and change from satellite radar altimetry and GRACE, 2003–2014. *J. Geophys. Res.*, **121**, 4303–4322, https://doi.org/10.1002/2015JC011579.

Bacon, S., G. Reverdin, I. G. Rigor, and H. M. Snaith, 2002: A freshwater jet on the east Greenland shelf. *J. Geophys. Res.*, **107**, C7-3068, https://doi.org/10.1029/2001JC000935.

Bacon, S., A. Marshall, N. P. Holliday, Y. Aksenov, and S. R. Dye, 2014: Seasonal variability of the East Greenland coastal current. *J. Geophys. Res.*, **119**, 3967–3987, https://doi.org/10.1002/2013JC009279.

Bacon, S., Y. Aksenov, S. Fawcett, and G. Madec, 2015: Arctic mass, freshwater and heat fluxes: methods and modelled seasonal variability. *Philos. Trans. Roy. Soc. A*, **373**, 20140169, https://doi.org/10.1098/rsta.2014.0169.

Downloaded from http://journals.ametsoc.org/jcli/article-pdf/doi/10.1175/JCLI-D-19-0083.1/4954456/jclid190083.pdf by UNIVERSITY OF SOUTHAMPTON HIGHFIELD user on 11 June 2020

Accepted for publication in *Journal of Climate*. DOI10.1175/JCLI-D-19-0083.1.

Barnier, B., and Coauthors, 2006: Impact of partial steps and momentum advection schemes in a global ocean circulation model at eddy-permitting resolution. *Ocean Dyn.*, **56**, 543–567, https://doi.org/10.1007/s10236-006-0082-1.

Becker, J. J., and Coauthors, 2009: Global bathymetry and elevation data at 30 arc seconds resolution: SRTM30_PLUS. *Mar. Geod.*, **32**, 355–371, https://doi.org/10.1080/01490410903297766.

Belkin, I. M., 2004: Propagation of the "Great Salinity Anomaly" of the 1990s around the northern North Atlantic. *Geophys. Res. Lett.*, **31**, L08306, https://doi.org/10.1029/2003GL019334.

Belkin, I. M., S. Levitus, J. Antonov, and S.-A. Malmberg, 1998: "Great Salinity Anomalies" in the North Atlantic. *Prog. Oceanogr.* **41**, 1-68, https://doi.org/10.1016/S0079-6611(98)00015-9.

Benetti, M., and Coauthors, 2017: Composition of freshwater in the spring of 2014 on the southern Labrador shelf and slope. *J. Geophys. Res.*, **122**, 1102–1121, https://doi.org/10.1002/2016JC012244.

Bouillon, S., M. A. Morales Maqueda, V. Legat, V., and T. Fichefet, 2009: An elastic-viscous-plastic sea ice model formulated on Arakawa B and C grids. *Ocean Modelling*, **27**, 174–184, https://doi.org/10.1016/j.ocemod.2009.01.004.

Boyer, T., S. Levitus, J. Antonov, R. Locarnini, A. Mishonov, H. Garcia, and S. A. Josey, 2007: Changes in freshwater content in the North Atlantic Ocean 1955–2006. *Geophys. Res. Lett.*, **34**, L16603, https://doi.org/10.1029/2007GL030126.

Brodeau, L., B. Barnier, A. M. Treguier, T. Penduff, and S. Gulev, 2010: An ERA40-based

Downloaded from http://journals.ametsoc.org/jcli/article-pdf/doi/10.1175/JCLI-D-19-0083.1/4954456/jclid190083.pdf by UNIVERSITY OF SOUTHAMPTON HIGHFIELD user on 11 June 2020

Accepted for publication in *Journal of Climate*. DOI10.1175/JCLI-D-19-0083.1.

atmospheric forcing for global ocean circulation models. *Ocean Modell.*, **31**, 88–104, https://doi.org/10.1016/j.ocemod.2009.10.005.

Broecker, W. S., 1991: The great ocean conveyor. *Oceanography,* **4**, 79-89, https://doi.org/10.5670/oceanog.1991.07

Carmack, E. C., 2000: The Arctic Ocean’s freshwater budget: sources, storage and export. *The freshwater budget of the Arctic Ocean*, E. L. Lewis et al., Eds., NATO Science Series 2: Environmental Security, Vol. 70, Springer, Dordrecht, 91–126, https://doi.org/10.1007/978-94-011-4132-1_5.

Carmack, E. C., 2007: The alpha/beta ocean distinction: A perspective on freshwater fluxes, convection, nutrients and productivity in high-latitude seas. *Deep-Sea Res. II*, **54**, 2578–2598, https://doi.org/10.1016/j.dsr2.2007.08.018.

Carmack, E. C., and Coauthors, 2016: Freshwater and its role in the Arctic marine system: sources, disposition, storage, export, and physical and biogeochemical consequences in the Arctic and global oceans. *J. Geophys. Res.*, **121**, 675-717, https://doi.org/10.1002/2015JG003140.

Colbourne, E. B., D. R. Senciall, and K. D. Foote, 1995: Temperature, salinity and sigma-t along the standard Seal Island transect. Canadian Technical Report of Hydrography and Ocean Sciences No. 164, 241 pp, http://publications.gc.ca/pub?id=9.805840&sl=0.

Colbourne, E., 2004: The history of standard hydrographic sections in Newfoundland and Labrador. *AZMP Bull.,* **4**, 29–33, http://www.meds-sdmm.dfo-mpo.gc.ca/isdm-gdsi/azmp-pmza/publications-eng.html.

Cuny, J., P. B. Rhines, P. P. Niiler, and S. Bacon, 2002: Labrador Sea boundary currents and

Downloaded from http://journals.ametsoc.org/jcli/article-pdf/doi/10.1175/JCLI-D-19-0083.1/4954456/jclid190083.pdf by UNIVERSITY OF SOUTHAMPTON HIGHFIELD user on 11 June 2020

Accepted for publication in *Journal of Climate*. DOI10.1175/JCLI-D-19-0083.1.

the fate of the Irminger Sea Water. *J. Phys. Oceanogr.*, **32**, 627–647, https://doi.org/10.1175/1520-0485(2002)032<0627:LSBCAT>2.0.CO;2.

Curry, R., and C. Mauritzen, 2005: Dilution of the northern North Atlantic Ocean in recent decades. *Science*, **308**, 1772–1774, https://doi.org/10.1126/science.1109477.

Curry, B., C. Lee, B. Petrie, R. Moritz, and R. Kwok, 2014: Multiyear volume, liquid freshwater, and sea ice transports through Davis Strait, 2004–10. *J. Phys. Oceanogr.*, **44**, 1244–1266, https://doi.org/10.1175/JPO-D-13-0177.1.

Déry, S. J., M. Stieglitz, E. C. McKenna, and E. F. Wood, 2005: Characteristics and Trends of River Discharge into Hudson, James, and Ungava bays, 1964–2000. *J. Climate*, **18**, 2540–2557, https://doi.org/10.1175/JCLI3440.1.

Déry, S. J., T. A. Stadnyk, M. K. MacDonald, and B. Gauli-Sharma, 2016: Recent trends and variability in river discharge across northern Canada. *Hydrol. Earth Syst. Sci.*, **20**, 4801–4818, https://doi.org/10.5194/hess-2016-461.

Dickson, R. R., J. Meincke, S. A. Malmberg, and A. J. Lee, 1988: The “great salinity anomaly” in the northern North Atlantic 1968–1982. *Prog. Oceanogr.*, **20**, 103–151, https://doi.org/10.1016/0079-6611(88)90049-3.

Dickson, R., B. Rudels, S. Dye, M. Karcher, J. Meincke, and I. Yashayaev, 2007: Current estimates of freshwater flux through Arctic and subarctic seas. *Prog. Oceanogr.*, **73**, 210–230, https://doi.org/10.1016/j.pocean.2006.12.003.

Drinkwater, K., 1986: Physical oceanography of Hudson Strait and Ungava Bay. *Canadian Inland Seas*, I. P. Martini, Ed., Elsevier, 237–264, https://doi.org/10.1016/S0422-9894(08)70906-1.

Downloaded from http://journals.ametsoc.org/jcli/article-pdf/doi/10.1175/JCLI-D-19-0083.1/4954456/jclid190083.pdf by UNIVERSITY OF SOUTHAMPTON HIGHFIELD user on 11 June 2020

Accepted for publication in *Journal of Climate*. DOI10.1175/JCLI-D-19-0083.1.

Drinkwater, K., 1988: On the mean and tidal currents in Hudson Strait. *Atmos.–Ocean*, **26**, 252–266, https://doi.org/10.1080/07055900.1988.9649302.

Fichefet, T., and M. A. Morales Maqueda, 1997: Sensitivity of a global sea ice model to the treatment of ice thermodynamics and dynamics. *J. Geophys. Res.*, **102**, 12609–12646, https://doi.org/10.1029/97JC00480.

Fofonoff, P., and R. C. Millard Jr., 1983: Algorithms for computation of fundamental properties of seawater. UNESCO Technical Papers in Marine Science 44, 53pp, http://hdl.handle.net/11329/109.

Giles, K. A., S. W. Laxon, A. L. Ridout, D. J. Wingham, and S. Bacon, 2012: Western Arctic Ocean freshwater storage increased by wind-driven spin-up of the Beaufort Gyre. *Nat. Geosci.*, **5**, 194–197, https://doi.org/10.1038/NGEO1379.

Good, S. A., M. J. Martin, and N. A. Rayner, 2013: EN4: Quality controlled ocean temperature and salinity profiles and monthly objective analyses with uncertainty estimates. *J. Geophys. Res.*, **118**, 6704–6716, https://doi.org/10.1002/2013JC009067.

Gouretski, V., and F. Reseghetti, 2010: On depth and temperature biases in bathythermograph data: Development of a new correction scheme based on analysis of a global ocean database. *Deep-Sea Res. I*, **57**, https://doi.org/10.1016/j.dsr.2010.03.011.

Haine, T. W., and Coauthors, 2015: Arctic freshwater export: status, mechanisms, and prospects. *Global Planet. Change*, **125**, 13–35, https://doi.org/10.1016/j.gloplacha.2014.11.013.

Häkkinen, S., 1993: An Arctic source for the great salinity anomaly: a simulation of the Arctic ice-ocean system for 1955–1975. *J. Geophys. Res.*, **98**, 16397–16410,

Downloaded from http://journals.ametsoc.org/jcli/article-pdf/doi/10.1175/JCLI-D-19-0083.1/4954456/jclid190083.pdf by UNIVERSITY OF SOUTHAMPTON HIGHFIELD user on 11 June 2020

Accepted for publication in *Journal of Climate*. DOI10.1175/JCLI-D-19-0083.1.

https://doi.org/10.1029/93JC01504.

Häkkinen, S., and A. Proshutinsky, 2004: Freshwater content variability in the Arctic Ocean. *J. Geophys. Res.*, **109,** C03051, https://doi.org/10.1029/2003JC001940.

Holliday, N. P., A. Meyer, S. Bacon, S. G. Alderson, and B. de Cuevas, 2007: Retroflection of part of the east Greenland current at Cape Farewell. *Geophys. Res. Lett.*, **34**, L07609, https://doi.org/10.1029/2006GL029085.

Holliday, N. P., S. Bacon, S. A. Cunningham, S. F. Gary, J. Karstensen, B. A. King, F. Li, and E. L. Mcdonagh, 2018: Subpolar North Atlantic overturning and gyre - scale circulation in the summers of 2014 and 2016. *J. Geophys. Res.*, 123, 4538–4559, https://doi.org/10.1029/2018JC013841.

Howatt, T., J. B. Palter, J. B. R. Matthews, B. DeYoung, R. Bachmayer and B. Claus, 2018: Ekman and Eddy Exchange of Freshwater and Oxygen across the Labrador Shelf Break. *J. Phys. Oceanogr.*, **48**, 1015-1031, https://doi.org/10.1175/JPO-D-17-0148.1.

Hunke, E. C., and J. K. Dukowicz, 1997: An elastic-viscous-plastic model for sea ice dynamics. *J. Phys. Oceanogr.*, **27**, 1849–1867, https://doi.org/10.1175/1520-0485(1997)027<1849:AEVPMF>2.0.CO;2.

Ingram, R., and S. Prinsenberg, 1998: Coastal oceanography of Hudson Bay and surrounding eastern Canadian Arctic waters. *The global coastal ocean: regional studies and synthesis, The Sea: Ideas and Observations on Progress in the Study of the Seas*, Vol. 11, 835–859.

Jackett, D.R. and T.J. Mcdougall, 1995: Minimal adjustment of hydrographic profiles to achieve static stability. *J. Atmos. Oceanic Technol.*, **12**, 381–389, https://doi.org/10.1175/1520-0426(1995)012<0381:MAOHPT>2.0.CO;2

Accepted for publication in *Journal of Climate*. DOI 10.1175/JCLI-D-19-0083.1.

Downloaded from http://journals.ametsoc.org/jcli/article-pdf/doi/10.1175/JCLI-D-19-0083.1/4954456/jclid190083.pdf by UNIVERSITY OF SOUTHAMPTON HIGHFIELD user on 11 June 2020

Jahn, A., B. Tremblay, L. A. Mysak, and R. Newton, 2010: Effect of the large-scale atmospheric circulation on the variability of the Arctic Ocean freshwater export. *Climate Dyn.*, **34**, 201–222, https://doi.org/10.1007/s00382-009-0558-z.

Jakobsson, M., 2002: Hypsometry and volume of the Arctic Ocean and its constituent seas. *Geochem. Geophys. Geosyst.*, **3**, 1–18, https://doi.org/10.1029/2001GC000302.

Jakobsson, M., R. Macnab, L. Mayer, R. Anderson, M. Edwards, J. Hatzky, H. W. Schenke, and P. Johnson, 2008: An improved bathymetric portrayal of the Arctic Ocean: implications for ocean modeling and geological, geophysical and oceanographic analyses. *Geophys. Res. Lett*., **35**, L07602, https://doi.org/10.1029/2008GL033520.

Josey, S. A. and R. Marsh, 2005: Surface freshwater flux variability and recent freshening of the North Atlantic in the eastern subpolar gyre. *J. Geophys. Res.*, **110**, C05008, https://doi.org/10.1029/2004JC002521.

Karcher, M., R. Gerdes, F. Kauker, C. Köberle, and I. Yashayaev, 2005: Arctic Ocean change heralds North Atlantic freshening. *Geophys. Res. Lett.*, **32**, L21606, https://doi.org/10.1029/2005GL023861.

Köberle, C., and R. Gerdes, 2007: Simulated variability of the Arctic Ocean freshwater balance 1948–2001. *J. Phys. Oceanogr.*, **37**, 1628–1644, https://doi.org/10.1175/JPO3063.1.

Kollmeyer, R. C., D. A. McGill, and N. Corwin, 1967: Oceanography of the Labrador Sea in the vicinity of Hudson Strait in 1965. US Coast Guard Oceanographic Report No. 12, 92pp, https://doi.org/10.5962/bhl.title.16966.

Lazier, J. R., and D. G. Wright, 1993: Annual velocity variations in the Labrador Current. *J. Phys. Oceanogr.*, **23**, 659–678, https://doi.org/10.1175/1520-

Downloaded from http://journals.ametsoc.org/jcli/article-pdf/doi/10.1175/JCLI-D-19-0083.1/4954456/jclid190083.pdf by UNIVERSITY OF SOUTHAMPTON HIGHFIELD user on 11 June 2020

Accepted for publication in *Journal of Climate*. DOI 10.1175/JCLI-D-19-0083.1.

0485(1993)023<0659:AVVITL>2.0.CO;2.

LeBlond, P. H., T. Osborn, D. Hodgins, R. Goodman, and M. Metge, 1981: Surface circulation in the western Labrador Sea. *Deep-Sea Res. A*, **28**, 683–693, https://doi.org/10.1016/0198-0149(81)90129-1.

Levier, B., A. M. Tréguier, G. Madec, and V. Garnier, 2007: Free surface and variable volume in the NEMO code. MERSEA IP report WP09-CNRS-STR03-1A, 47pp,

Levitus, S., 1989: Interpentadal variability of temperature and salinity at intermediate depths of the North Atlantic Ocean, 1970–1974 versus 1955–1959. *J. Geophys. Res.*, **94**, 6091–6131, https://doi.org/10.1029/JC094iC05p06091.

Lique, C., A. M. Treguier, M. Scheinert, and T. Penduff, 2009: A model-based study of ice and freshwater transport variability along both sides of Greenland. *Climate Dyn.*, **33**, 685–705, https://doi.org/10.1007/s00382-008-0510-7.

Lique, C., and M. Steele, 2012: Where can we find a seasonal cycle of the Atlantic water temperature within the Arctic Basin? *J. Geophys. Res.*, **117**, C03026, https://doi.org/10.1029/2011JC007612.

Lozier, S., and Coauthors, 2017: Overturning in the Subpolar North Atlantic Program: a new international ocean observing system. *Bull. Amer. Meteor. Soc.*, **98**, 737–752, https://doi.org/10.1175/BAMS-D-16-0057.1.

Lozier, S., and Coauthors, 2019: A sea change in our view of overturning in the Subpolar North Atlantic. *Science*, **363**, 516-521, https://doi.org/10.1126/science.aau6592.

Macrander, A., H. Valdimarsson, and S. Jónsson, 2014: Improved transport estimate of the East Icelandic Current 2002–2012. *J. Geophys. Res.*, **119**, 3407–3424,

Downloaded from http://journals.ametsoc.org/jcli/article-pdf/doi/10.1175/JCLI-D-19-0083.1/4954456/jclid190083.pdf by UNIVERSITY OF SOUTHAMPTON HIGHFIELD user on 11 June 2020

Accepted for publication in *Journal of Climate*. DOI 10.1175/JCLI-D-19-0083.1.

https://doi.org/10.1002/2013JC009517.

Madec, G., and the NEMO team, 2016: *NEMO ocean engine*. Note du Pôle de modélisation de l'Institut Pierre-Simon Laplace No 27, 386pp, ISSN No 1288–1619.

Manabe, S., and R. J. Stouffer, 1995: Simulation of abrupt climate change induced by freshwater input to the North Atlantic Ocean. *Nature*, **378**, 165–167, https://doi.org/10.1038/378165a0.

Martin, T., M. Tsamados, D. Schroeder, and D. L. Feltham, 2016: The impact of variable sea ice roughness on changes in Arctic Ocean surface stress: a model study. *J. Geophys. Res.*, **121**, 1931–1952, https://doi.org/10.1002/2015JC011186.

Marzocchi, A., J. J. M. Hirschi, N. P. Holliday, S. A. Cunningham, A. T. Blaker, and A. C. Coward, 2015: The North Atlantic subpolar circulation in an eddy-resolving global ocean model. *J. Mar. Syst.*, **142**, 126–143, https://doi.org/10.1016/j.jmarsys.2014.10.007.

McDougall, T. J., and P. M. Barker, 2011: Getting started with TEOS-10 and the Gibbs seawater (GSW) oceanographic toolbox. Rep. SCOR/IAPSO WG127, 28 pp., https://doi.org/10.1002/2014JC010066, available at www.TEOS-10.org.

Mertz, G., S. Narayanan, and J. Helbig, 1993: The freshwater transport of the Labrador Current. *Atmosphere-Ocean*, **31**, 281-295, https://doi.org/10.1080/07055900.1993.9649472.

Myers, R. A., S. A. Akenhead, and K. Drinkwater, 1990: The influence of Hudson Bay runoff and ice melt on the salinity of the inner Newfoundland shelf. *Atmosphere-Ocean*, **28**, 241-256, https://doi.org/10.1080/07055900.1990.9649377.

National Geophysical Data Center, 2006: 2-minute gridded global relief data (ETOPO2) v2. Geo-physical Data Center, NOAA, https://doi.org/10.7289/V5J1012Q.

Downloaded from http://journals.ametsoc.org/jcli/article-pdf/doi/10.1175/JCLI-D-19-0083.1/4954456/jclid190083.pdf by UNIVERSITY OF SOUTHAMPTON HIGHFIELD user on 11 June 2020

Accepted for publication in *Journal of Climate*. DOI10.1175/JCLI-D-19-0083.1.

Nurser, A., and S. Bacon, 2014: The Rossby radius in the Arctic Ocean. *Ocean Sci.*, **10**, 967–975, https://doi.org/10.5194/os-10-967-2014.

Peterson, B. J., J. McClelland, R. Curry, R. M. Holmes, J. E. Walsh, and K. Aagaard, 2006: Trajectory shifts in the Arctic and subarctic freshwater cycle. *Science*, **313**, 1061–1066, https://doi.org/10.1126/science.1122593.

Petrie, B., S. Akenhead, S. Lazier, and J. Loder, 1988: The cold intermediate layer on the Labrador and northeast Newfoundland shelves, 1978–86. *NAFO Sci. Counc. Stud.*, **12**, 57–69, https://archive.nafo.int/open/studies/s12/petrie.pdf.

Polyakov, I. V., and Coauthors, 2008: Arctic Ocean freshwater changes over the past 100 years and their causes. *J. Climate*, **21**, 364–384, https://doi.org/10.1175/2007JCLI1748.1.

Polyakov, I. V., U. S. Bhatt, J. E. Walsh, E. P. Abrahamsen, A. V. Pnyushkov, and P. F. Wassmann, 2013: Recent oceanic changes in the Arctic in the context of long-term observations. *Ecol. Appl.*, **23**, 1745–1764, https://doi.org/10.1890/11-0902.1.

Prinsenberg, S., and J. Hamilton, 2005: Monitoring the volume, freshwater and heat fluxes passing through Lancaster Sound in the Canadian Arctic Archipelago. *Atmosphere-Ocean*, **43**, 1–22, https://doi.org/10.3137/ao.430101.

Proshutinsky, A. Y., and M. A. Johnson, 1997: Two circulation regimes of the wind-driven Arctic Ocean. *J. Geophys. Res.*, **102**, 12493–12514, https://doi.org/10.1029/97JC00738.

Proshutinsky, A., R. Bourke, and F. McLaughlin, 2002: The role of the Beaufort Gyre in Arctic climate variability: seasonal to decadal climate scales. *Geophys. Res. Lett.*, **29**, 15-1–15-4, https://doi.org/10.1029/2002GL015847.

Proshutinsky, A., and Coauthors, 2009: Beaufort Gyre freshwater reservoir: state and

Downloaded from http://journals.ametsoc.org/jcli/article-pdf/doi/10.1175/JCLI-D-19-0083.1/4954456/jclid190083.pdf by UNIVERSITY OF SOUTHAMPTON HIGHFIELD user on 11 June 2020

Accepted for publication in *Journal of Climate*. DOI10.1175/JCLI-D-19-0083.1.

variability from observations. *J. Geophys. Res.*, **114**, C00A10, https://doi.org/10.1029/2008JC005104.

Proshutinsky, A., D. Dukhovskoy, M. L. Timmermans, R. Krishfield, and J. L. Bamber, 2015: Arctic circulation regimes. *Philos. Trans. Roy. Soc. A*, **373**, 20140160, https://doi.org/10.1098/rsta.2014.0160.

Rabe, B., and Coauthors, 2013: Liquid export of Arctic freshwater components through the Fram Strait 1998–2011. *Ocean Sci.*, **9**, 91–109, https://doi.org/10.5194/os-9-91-2013.

Rabe, B., and Coauthors, 2014: Arctic Ocean basin liquid freshwater storage trend 1992–2012. *Geophys. Res. Lett.*, **41**, 961–968, https://doi.org/10.1002/2013GL058121.

Ridenour, N. A., X. Hu, K. Sydor, P. G. Myers, and D. G. Barber, 2019: Revisiting the circulation of Hudson Bay: evidence for a seasonal pattern. *Geophys. Res. Lett.*, **46**, https://doi.org/10.1029/2019GL082344.

Rudels, B., E. Fahrbach, J. Meincke, G. Budéus, and P. Eriksson, 2002: The East Greenland Current and its contribution to the Denmark Strait overflow. *ICES J. Mar. Sci.*, **59**, 1133–1154, https://doi.org/10.1006/jmsc.2002.1284.

Schauer, U. and M. Losch, 2019: Freshwater in the ocean is not a useful parameter in climate research. *J. Phys. Oceanogr.*, **49**, 2309-2321, https://doi.org/10.1175/JPO-D-19-0102.1.

Skagseth, Ø., K. F. Drinkwater, and E. Terrile, 2011: Wind-and buoyancy-induced transport of the Norwegian Coastal Current in the Barents Sea. *J. Geophys. Res.*, **116**, C08007, https://doi.org/10.1029/2011JC006996.

Smith, E. H., F. M. Soule, and O. Mosby, 1937: *The Marion and General Greene expeditions to the Davis Strait and Labrador Sea under direction of the United States Coast Guard, 1928-*

Downloaded from http://journals.ametsoc.org/jcli/article-pdf/doi/10.1175/JCLI-D-19-0083.1/4954456/jclid190083.pdf by UNIVERSITY OF SOUTHAMPTON HIGHFIELD user on 11 June 2020

Accepted for publication in *Journal of Climate*. DOI10.1175/JCLI-D-19-0083.1.

1931-1933-1934-1935. Scientific Results Part 2, Physical Oceanography. US Government Printing Office, https://doi.org/10.5962/bhl.title.10182.

Smith, W. H. F., and D. T. Sandwell, 1997: Global seafloor topography from satellite altimetry and ship depth soundings: evidence for stochastic reheating of the oceanic lithosphere. *Science*, **277**, 1956–1962, https://doi.org/10.1126/science.277.5334.1956.

Smith, W. H. F., and D. T. Sandwell, 2004: Conventional bathymetry, bathymetry from space, and geodetic altimetry. *Oceanography*, **17**, 8–23, https://doi.org/10.5670/oceanog.2004.63.

Spreen, G., S. Kern, D. Stammer, and E. Hansen, 2009: Fram Strait sea ice volume export estimated between 2003 and 2008 from satellite data. *Geophys. Res. Lett.,* **36**, L19502, https://doi.org/10.1029/2009GL039591.

Steele, M., R. Morley, and W. Ermold, 2001: PHC: a global ocean hydrography with a high-quality Arctic Ocean. *J. Climate*, **14**, 2079–2087, https://doi.org/10.1175/1520-0442(2001)014<2079:PAGOHW>2.0.CO;2.

de Steur, L., E. Hansen, R. Gerdes, M. Karcher, E. Fahrbach, and J. Holfort, 2009: Freshwater fluxes in the East Greenland Current: a decade of observations. *Geophys. Res. Lett.*, **36**, L23611, https://doi.org/10.1029/2009GL041278.

Straneo, F., and F. Saucier, 2008: The outflow from Hudson Strait and its contribution to the Labrador Current. *Deep-Sea Res. I*, **55**, 926– 946, https://doi.org/10.1016/j.dsr.2008.03.012.

Sundby, S., and K. Drinkwater, 2007: On the mechanisms behind salinity anomaly signals of the northern North Atlantic. *Prog. Oceanogr.* **73**, 190-202, https://doi:org/10.1016/j.pocean.2007.02.002.

Downloaded from http://journals.ametsoc.org/jcli/article-pdf/doi/10.1175/JCLI-D-19-0083.1/4954456/jclid190083.pdf by UNIVERSITY OF SOUTHAMPTON HIGHFIELD user on 11 June 2020

Accepted for publication in *Journal of Climate*. DOI10.1175/JCLI-D-19-0083.1.

Tang, C. C., C. K. Ross, T. Yao, B. Petrie, B. M. DeTracey, and E. Dunlap, 2004: The circulation, water masses and sea-ice of Baffin Bay. *Prog. Oceanogr.*, **63**, 183–228, https://doi.org/10.1016/j.pocean.2004.09.005.

Templeman, W., 1975: Comparison of temperatures in July-August hydrographic sections of the eastern Newfoundland area in 1972 and 1973 with those from 1951 to 1971. *ICNAF Special Publications*, **10**, 17–39, https://www.nafo.int/Library/ICNAF/ICNAF-Publications/ICNAF-Special-Publications/special-publication-no-10-issued-november-1975.

Thompson, D. W. J., and J. M. Wallace, 1998: The Arctic Oscillation signature in the wintertime geopotential height and temperature fields. *Geophys. Res. Lett.*, **25**, 1297–1300, https://doi.org/10.1029/98GL00950.

Thomson, R. E., and W. J. Emery, 2014: *Data analysis methods in physical oceanography*. Newnes, 728 pp.

Tsamados, M., D. L. Feltham, D. Schroeder, D. Flocco, S. L. Farrell, N. Kurtz, S. W. Laxon, and S. Bacon, 2014: Impact of variable atmospheric and oceanic form drag on simulations of Arctic Sea Ice. *J. Phys. Oceanogr.*, **44**, 1329–1353, https://doi.org/10.1175/JPO-D-13-0215.1.

Tsubouchi, T., and Coauthors, 2012: The Arctic Ocean in summer: a quasi-synoptic inverse estimate of boundary fluxes and water mass transformation. *J. Geophys. Res.*, **117**, C01024, https://doi.org/10.1029/2011JC007174.

Tsubouchi, T., and Coauthors, 2018: The Arctic Ocean seasonal cycles of heat and freshwater fluxes: observation-based inverse estimates. *J. Phys. Oceanogr.*, **48**, 2029–2055, https://doi.org/10.1175/JPO-D-17-0239.1.

Downloaded from http://journals.ametsoc.org/jcli/article-pdf/doi/10.1175/JCLI-D-19-0083.1/4954456/jclid190083.pdf by UNIVERSITY OF SOUTHAMPTON HIGHFIELD user on 11 June 2020

Accepted for publication in *Journal of Climate*. DOI10.1175/JCLI-D-19-0083.1.

Table 1. Seawater transport statistics (Sv) at the Seal Island section for Hudson outflow and LC-Arctic water, for 1/12º NEMO model in summertime (1995-2010) derived from 5-day means, and for measured section geostrophic velocities, referenced to zero at the bottom (Measured (0)) and to 1/12º NEMO model bottom velocities (Measured (NEMO)).

	Hudson outflow		LC-Arctic	
	Mean	sd	Mean	sd
NEMO 1/12º	0.28	0.08	1.19	0.32
Measured (0)	0.34	0.14	0.81	0.28
Measured (NEMO)	0.60	0.20	1.87	0.67

Table A1. Seal Island section standard station positions: original (1–9) and extended, from 1993 (10–14).

Station Number	Longitude (ºW)	Latitude (ºN)
1	55.65	53.23
2	55.50	53.33
3	55.00	53.62
4	54.50	53.92
5	54.00	54.20
6	53.50	54.50
7	53.25	54.63
8	53.00	54.78
9	52.50	55.07
10	55.36	53.41
11	55.15	53.53
12	54.78	53.75
13	54.22	54.08
14	53.73	54.35

Downloaded from http://journals.ametsoc.org/jcli/article-pdf/doi/10.1175/JCLI-D-19-0083.1/4954456/jclid190083.pdf by UNIVERSITY OF SOUTHAMPTON HIGHFIELD user on 11 June 2020

Accepted for publication in *Journal of Climate*. DOI10.1175/JCLI-D-19-0083.1.

Figure Captions

Figure 1. Main panel: study region, with key locations labelled; also James Bay (JB), Ungava Bay (UB), Fury and Hecla Strait (F&H). Solid lines show: locations of Davis and Hudson Strait sections (black) and the Seal Island section (maroon); indicative pathways of the Hudson outflow (orange), the continuation of the Baffin Island Current (yellow) and the recirculating Atlantic waters (red). Inset: Seal Island standard station positions. Selected depth contours (m) are labelled.

Figure 2. Measured (a-d) and modelled (e-h) summertime (July-August) mean (1995-2010) sections at Seal Island; temperature (ºC; a, e), salinity (b, f), density anomaly (kg m^{-3}; c, g), velocity (negative southwards; m s^{-1}; d, h). Measured panels include maximum and minimum densities corresponding to CIL temperatures –1 ºC (dashed line), 0 ºC (solid black line) and 1 ºC (dotted line); modelled panels show densities derived from velocity criteria; see text for details.

Figure 3. NEMO mean (1997-2007) surface salinity (a), temperature (ºC) at CIL core (61 m depth; b) and surface current speed (m s^{-1}; c).

Figure 4. NEMO summertime (1995-2010) mean velocities across the Seal Island section. (a) velocity (southwards negative; colours), salinity (thin black and dotted contours; contour interval 0.5, except for 35.1) and density anomaly (two contours, bold black, kg m^{-3}) versus depth; volume transport (Sv; white) accumulated towards the coast from zero offshore. (b) ratio of bottom velocity to surface velocity (red). (c) surface (black solid) and bottom (black dotted) velocities (southwards negative; m s^{-1}). The double vertical line shows the mean offshore limit of the LC-Arctic waters.

Figure 5. (a), (b) Montgomery potential (M, m^2 s^{-2}) and temperature (T, ºC) on the r_B = 25.0

Accepted for publication in *Journal of Climate*. DOI10.1175/JCLI-D-19-0083.1.

Downloaded from http://journals.ametsoc.org/jcli/article-pdf/doi/10.1175/JCLI-D-19-0083.1/4954456/jclid190083.pdf by UNIVERSITY OF SOUTHAMPTON HIGHFIELD user on 11 June 2020

kg m^{-3} pseudo-density surface (respectively), illustrating the source and spatial extent of the Hudson outflow; (c), (d) as (a), (b) for the r_B = 26.5 kg m^{-3} surface, for the LC-Arctic waters. Grey regions show where r_B surfaces ground into the sea floor or outcrop to the sea surface; latitude (ºN), longitude (ºW).

Figure 6. NEMO 1/12º model freshwater transports. (a) Time series of monthly (lines) and annual (circles) means (1995–2010): Davis Strait liquid (blue, solid) and ice (blue, dotted), and Seal Island LC-Arctic (orange) freshwater transports; Hudson Strait (green) and Seal Island Hudson outflow (red) freshwater transports (mSv). (b) Seasonal cycles per calendar month from data in (a) (±1 sd), except Davis Strait liquid and sea ice combined.

Figure 7. Seal Island freshwater flux in the Hudson outflow (a): annual (summertime) values (+), 7-year running average (black solid), record mean 57 mSv (horizontal dashed). Lagged sum of annual mean regional Canadian river runoff values (b): yearly values (+), 7-year running average (black solid), record mean 23 mSv (horizontal dashed); see text for details.

Figure 8. Seal Island LC-Arctic measured freshwater fluxes (mSv) 1950–2016 from summertime (Jul-Aug) sections. (a) total freshwater fluxes using 0 ºC CIL definition: yearly values (+); record mean 137 mSv (dashed line); 7-year running average (black), with periods above (below) the mean shown as blue (red) shaded areas; see text for derivation of (constant) current offsets from NEMO. (b) freshwater flux anomalies (zero mean) for the three CIL definitions CIL (–1, 0 and 1 ºC: key); yearly values (dashed); 7-year running average (solid).

Figure 9. Arctic freshwater export flux anomaly (mSv; Seal Island LC-Arctic flux anomaly using 0 ºC CIL definition, 7-year running average, as Figure 9b; black); Subpolar North Atlantic freshwater content (FWC; km^3) anomaly (blue); Arctic FWC anomaly from

Accepted for publication in *Journal of Climate*. DOI10.1175/JCLI-D-19-0083.1.

Downloaded from http://journals.ametsoc.org/jcli/article-pdf/doi/10.1175/JCLI-D-19-0083.1/4954456/jclid190083.pdf by UNIVERSITY OF SOUTHAMPTON HIGHFIELD user on 11 June 2020

Polyakov et al. (2013) as a 7-year running average (orange).

Downloaded from http://journals.ametsoc.org/jcli/article-pdf/doi/10.1175/JCLI-D-19-0083.1/4954456/jclid190083.pdf by UNIVERSITY OF SOUTHAMPTON HIGHFIELD user on 11 June 2020

Accepted for publication in *Journal of Climate*. DOI10.1175/JCLI-D-19-0083.1.

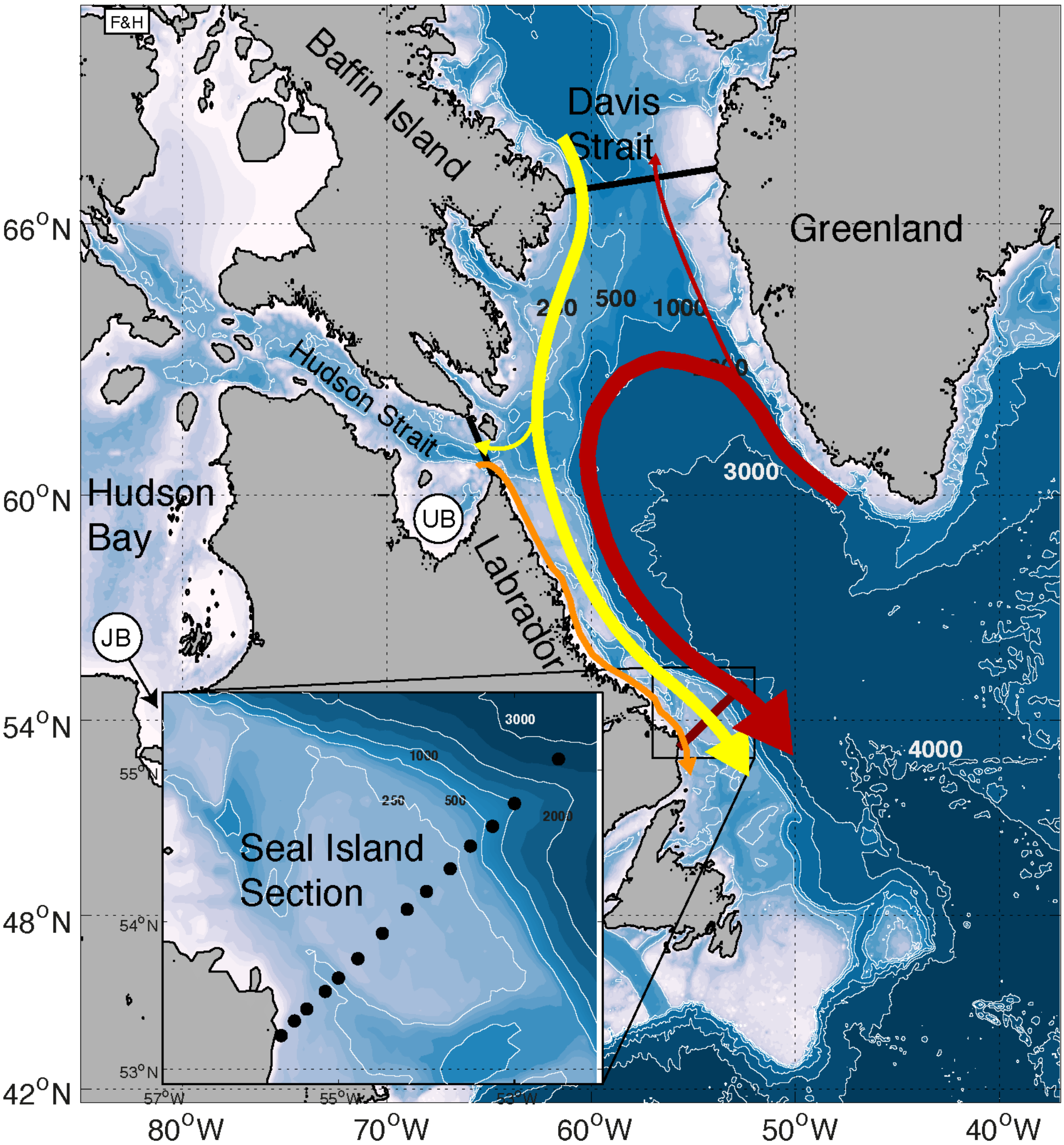

Figure 1. Main panel: study region, with key locations labelled; also James Bay (JB), Ungava Bay (UB), Fury and Hecla Strait (F&H). Solid lines show: locations of Davis and Hudson Strait sections (black) and the Seal Island section (maroon); indicative pathways of the Hudson outflow (orange), the continuation of the Baffin Island Current (yellow) and the recirculating Atlantic waters (red). Inset: Seal Island standard station positions. Selected depth contours (m) are labelled.

Downloaded from http://journals.ametsoc.org/jcli/article-pdf/doi/10.1175/JCLI-D-19-0083.1/4954456/jclid190083.pdf by UNIVERSITY OF SOUTHAMPTON HIGHFIELD user on 11 June 2020

Accepted for publication in *Journal of Climate*. DOI10.1175/JCLI-D-19-0083.1.

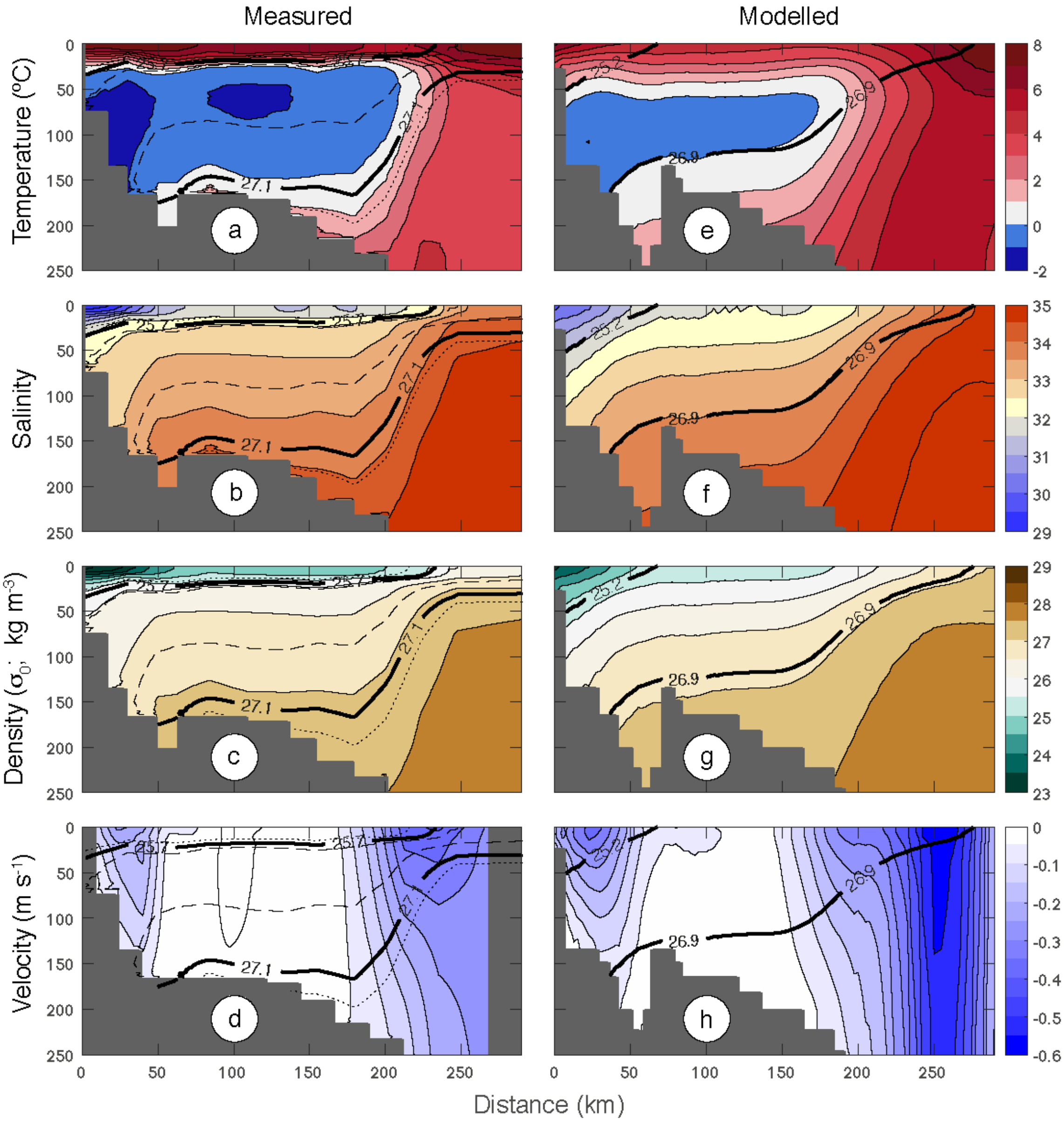

Figure 2. Measured (a-d) and modelled (e-h) summertime (July-August) mean (1995-2010) sections at Seal Island; temperature (ºC; a, e), salinity (b, f), density anomaly (kg m^{-3}; c, g), velocity (negative southwards; m s^{-1}; d, h). Measured panels include maximum and minimum densities corresponding to CIL temperatures –1 ºC (dashed line), 0 ºC (solid black line) and 1 ºC (dotted line); modelled panels show densities derived from velocity criteria; see text for details.

1157

Downloaded from http://journals.ametsoc.org/jcli/article-pdf/doi/10.1175/JCLI-D-19-0083.1/4954456/jclid190083.pdf by UNIVERSITY OF SOUTHAMPTON HIGHFIELD user on 11 June 2020

Accepted for publication in *Journal of Climate*. DOI10.1175/JCLI-D-19-0083.1.

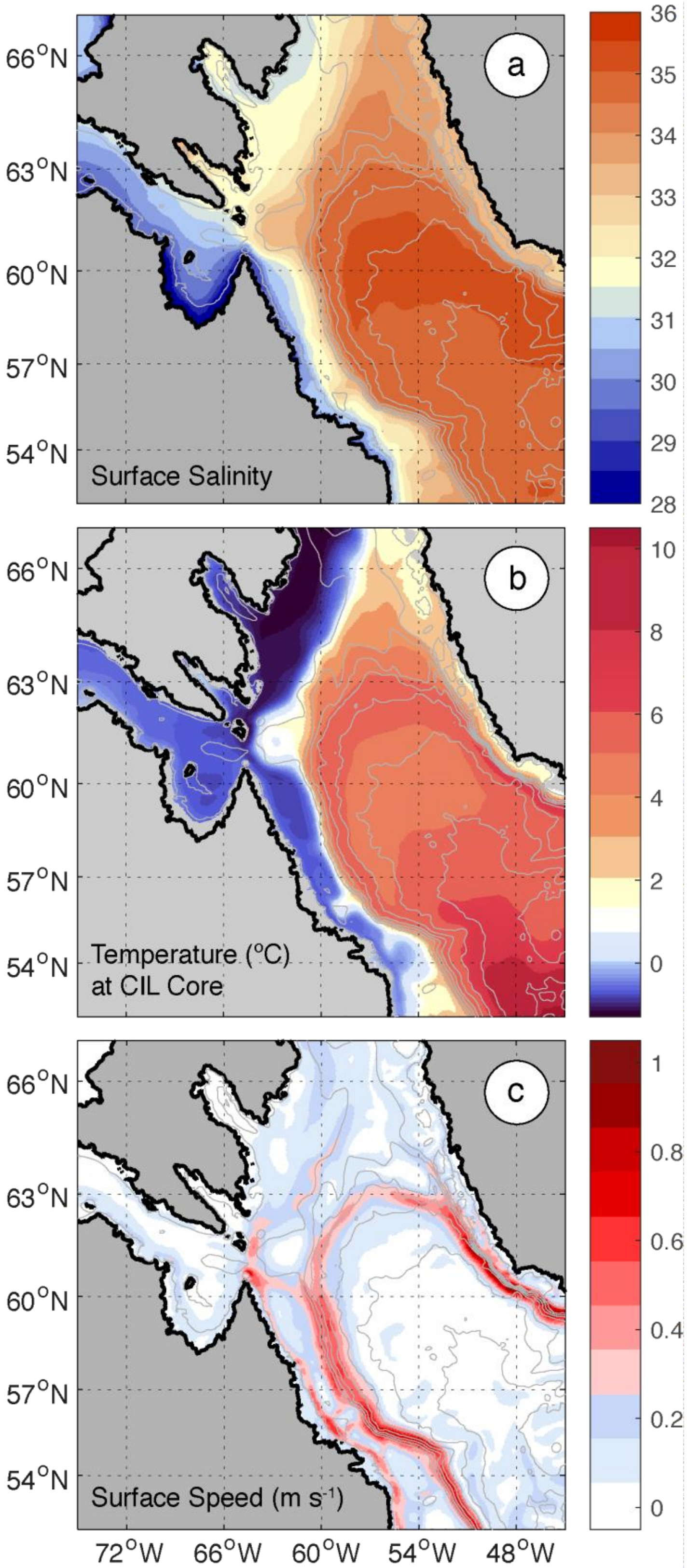

Figure 3. NEMO mean (1997-2007) surface salinity (a), temperature (ºC) at CIL core (61 m depth; b) and surface current speed (m s^{-1}; c).

1158

Downloaded from http://journals.ametsoc.org/jcli/article-pdf/doi/10.1175/JCLI-D-19-0083.1/4954456/jclid190083.pdf by UNIVERSITY OF SOUTHAMPTON HIGHFIELD user on 11 June 2020

Accepted for publication in *Journal of Climate*. DOI10.1175/JCLI-D-19-0083.1.

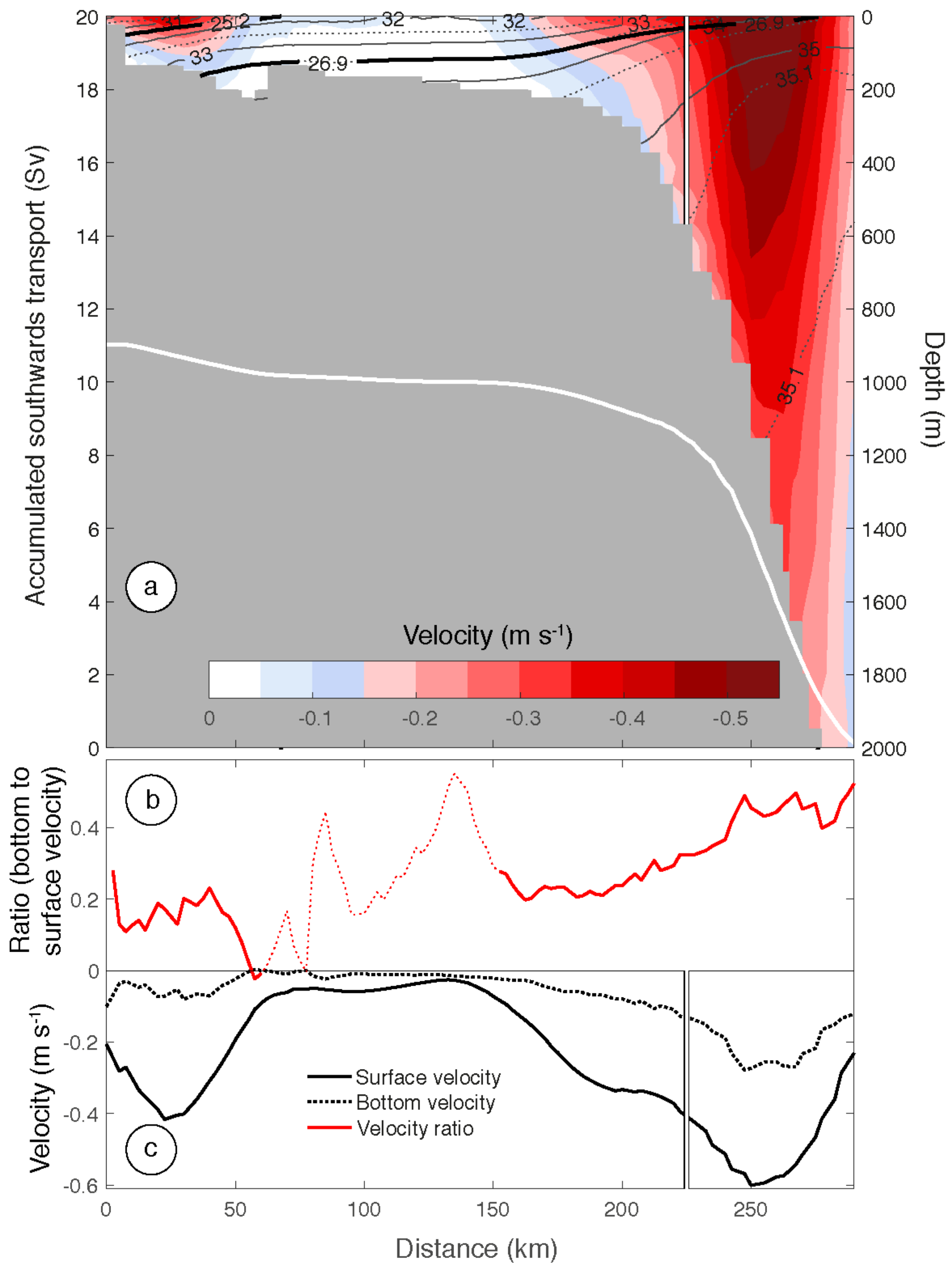

Figure 4. NEMO summertime (1995-2010) mean velocities across the Seal Island section. (a) velocity (southwards negative; colours), salinity (thin black and dotted contours; contour interval 0.5, except for 35.1) and density anomaly (two contours, bold black, kg m^{-3}) versus depth; volume transport (Sv; white) accumulated towards the coast from zero offshore. (b) ratio of bottom velocity to surface velocity (red). (c) surface (black solid) and bottom (black dotted) velocities (southwards negative; m s^{-1}). The double vertical line shows the mean offshore limit of the LC-Arctic waters.

1159

Accepted for publication in *Journal of Climate*. DOI10.1175/JCLI-D-19-0083.1.

Downloaded from http://journals.ametsoc.org/jcli/article-pdf/doi/10.1175/JCLI-D-19-0083.1/4954456/jclid190083.pdf by UNIVERSITY OF SOUTHAMPTON HIGHFIELD user on 11 June 2020

1160

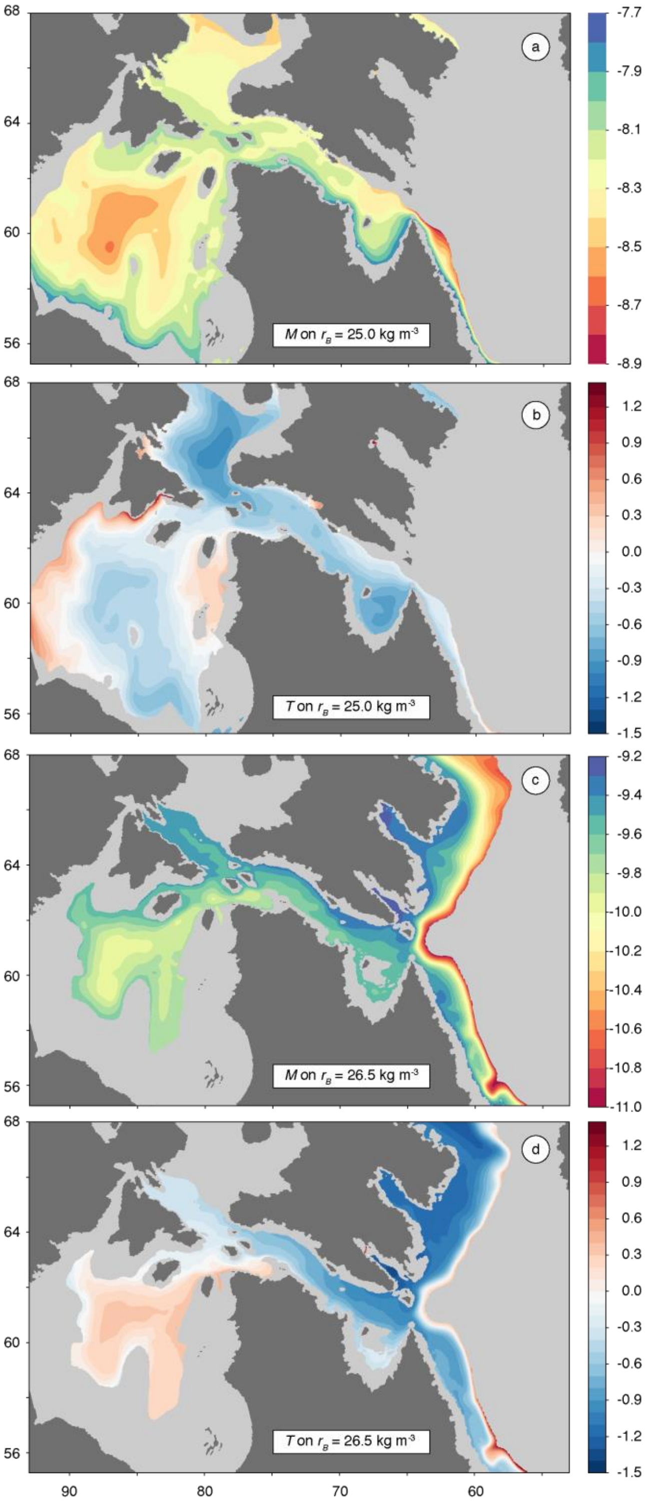

Figure 5. (a), (b) Montgomery potential (M, m^2 s^{-2}) and temperature (T, ºC) on the r_B = 25.0 kg m^{-3} pseudo-density surface (respectively), illustrating the source and spatial extent of the Hudson outflow; (c), (d) as (a), (b) for the r_B = 26.5 kg m^{-3} surface, for the LC-Arctic waters. Grey regions show where r_B surfaces ground into the sea floor or outcrop to the sea surface; latitude (ºN), longitude (ºW).

1161
1162

Accepted for publication in *Journal of Climate*. DOI10.1175/JCLI-D-19-0083.1.

Downloaded from http://journals.ametsoc.org/jcli/article-pdf/doi/10.1175/JCLI-D-19-0083.1/4954456/jclid190083.pdf by UNIVERSITY OF SOUTHAMPTON HIGHFIELD user on 11 June 2020

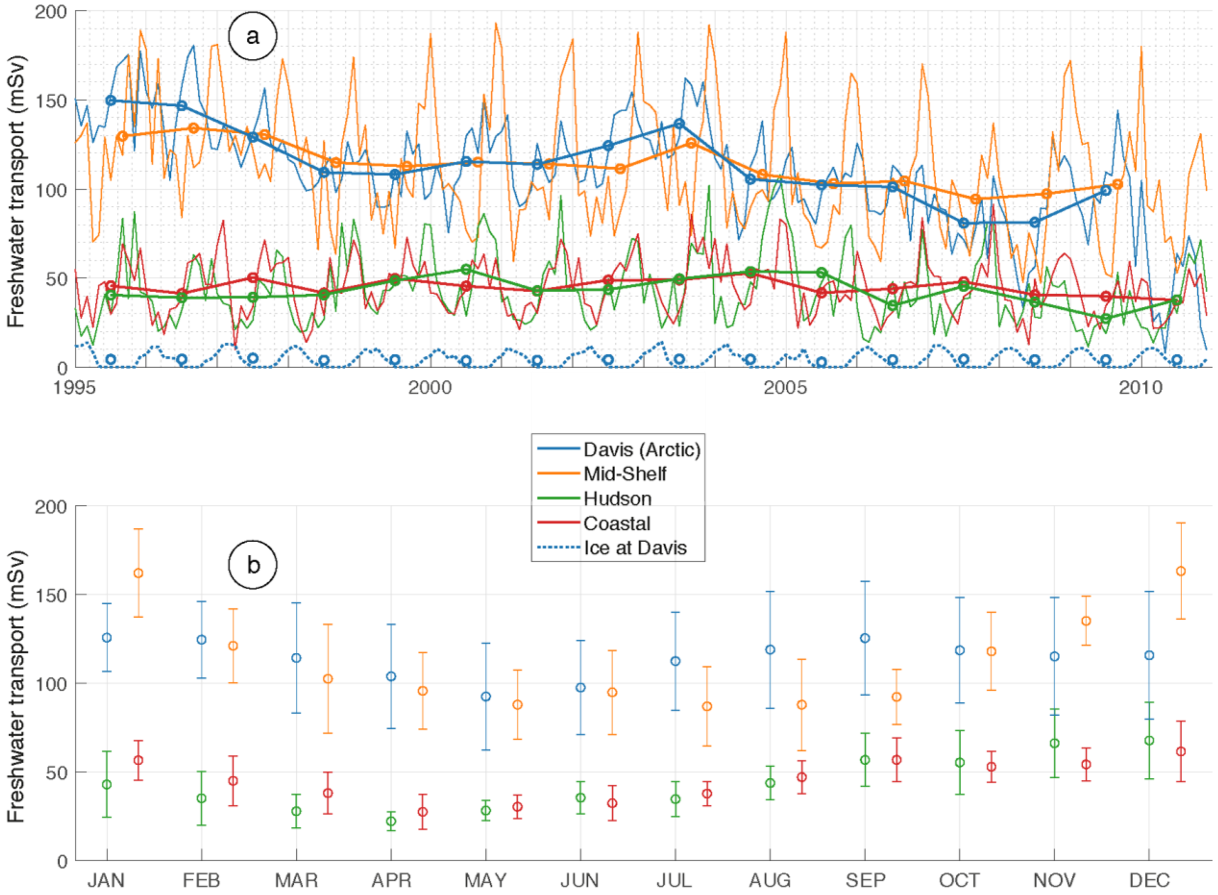

Figure 6. NEMO 1/12° model freshwater transports. (a) Time series of monthly (lines) and annual (circles) means (1995–2010): Davis Strait liquid (blue, solid) and ice (blue, dotted), and Seal Island LC-Arctic (orange) freshwater transports; Hudson Strait (green) and Seal Island Hudson outflow (red) freshwater transports (mSv). (b) Seasonal cycles per calendar month from data in (a) (±1 sd), except Davis Strait liquid and sea ice combined.

1163

Accepted for publication in *Journal of Climate*. DOI10.1175/JCLI-D-19-0083.1.

Downloaded from http://journals.ametsoc.org/jcli/article-pdf/doi/10.1175/JCLI-D-19-0083.1/4954456/jclid190083.pdf by UNIVERSITY OF SOUTHAMPTON HIGHFIELD user on 11 June 2020

1164

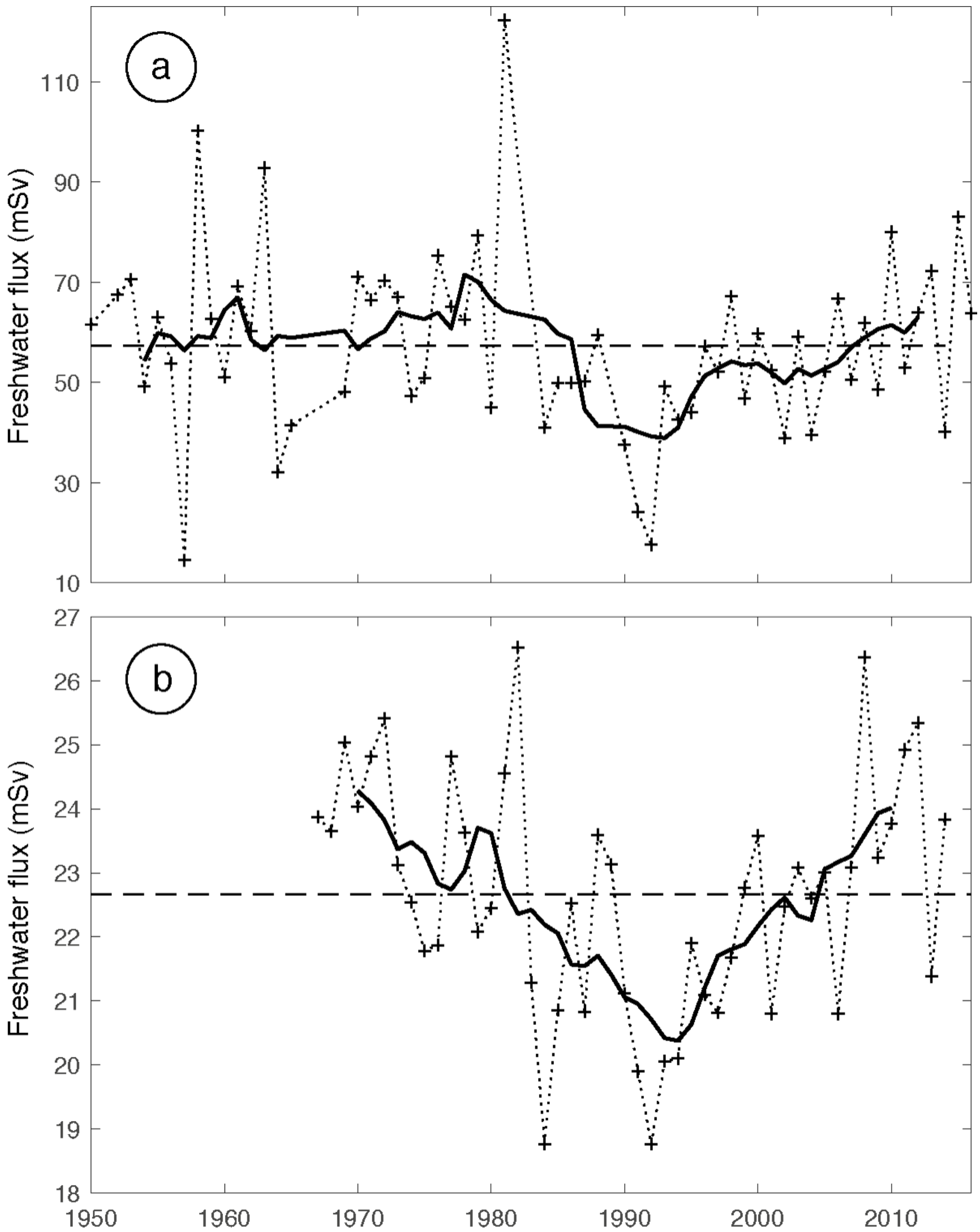

Figure 7. Seal Island freshwater flux in the Hudson outflow (a): annual (summertime) values (+), 7-year running average (black solid), record mean 57 mSv (horizontal dashed). Lagged sum of annual mean regional Canadian river runoff values (b): yearly values (+), 7-year running average (black solid), record mean 23 mSv (horizontal dashed); see text for details.

1165

Downloaded from http://journals.ametsoc.org/jcli/article-pdf/doi/10.1175/JCLI-D-19-0083.1/4954456/jclid190083.pdf by UNIVERSITY OF SOUTHAMPTON HIGHFIELD user on 11 June 2020

Accepted for publication in *Journal of Climate*. DOI10.1175/JCLI-D-19-0083.1.

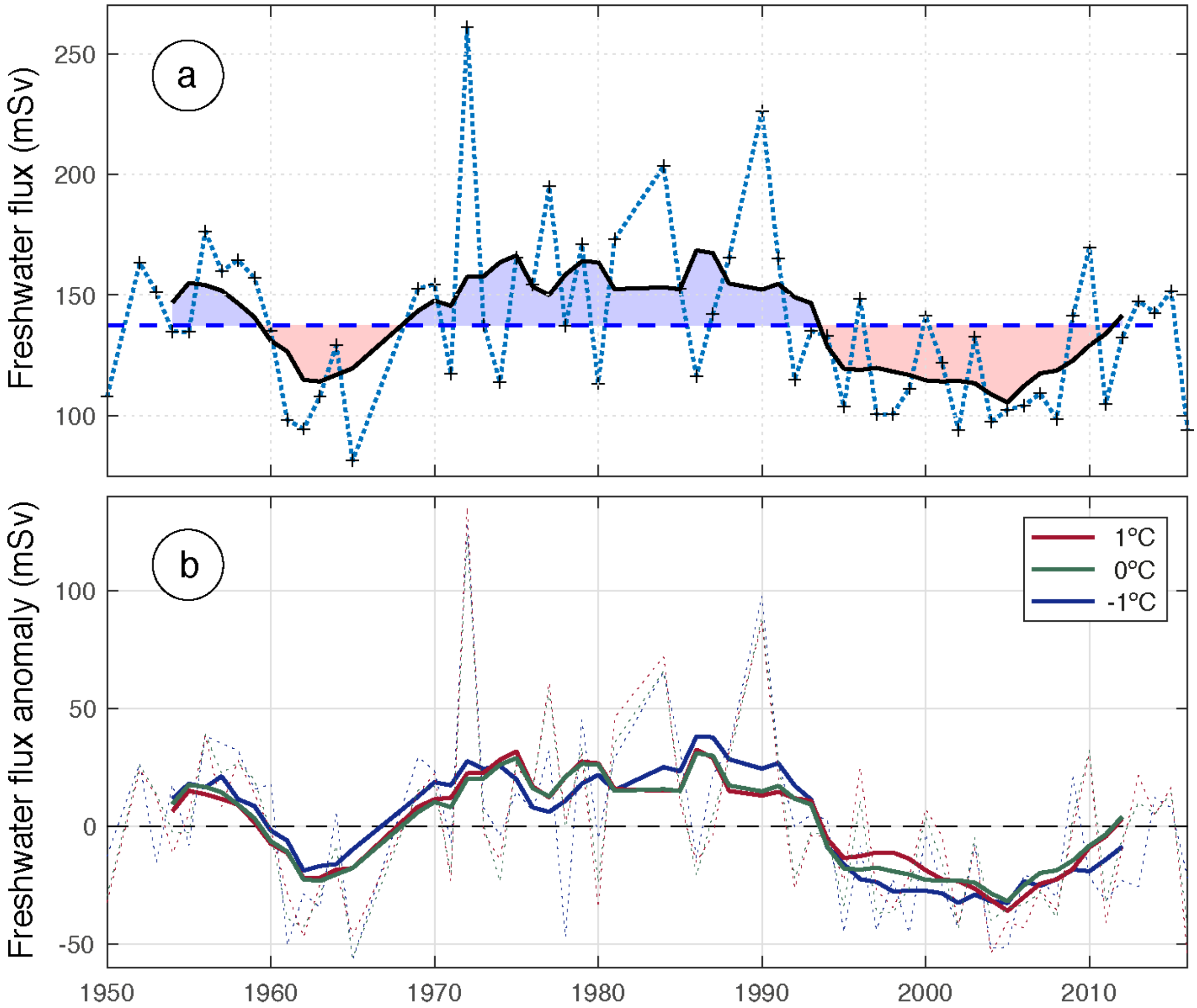

Figure 8. Seal Island LC-Arctic measured freshwater fluxes (mSv) 1950–2016 from summertime (Jul-Aug) sections. (a) total freshwater fluxes using 0 ºC CIL definition: yearly values (+); record mean 137 mSv (dashed line); 7-year running average (black), with periods above (below) the mean shown as blue (red) shaded areas; see text for derivation of (constant) current offsets from NEMO. (b) freshwater flux anomalies (zero mean) for the three CIL definitions CIL (–1, 0 and 1 ºC: key); yearly values (dashed); 7-year running average (solid).

1166

Downloaded from http://journals.ametsoc.org/jcli/article-pdf/doi/10.1175/JCLI-D-19-0083.1/4954456/jclid190083.pdf by UNIVERSITY OF SOUTHAMPTON HIGHFIELD user on 11 June 2020

Accepted for publication in *Journal of Climate*. DOI10.1175/JCLI-D-19-0083.1.

1167

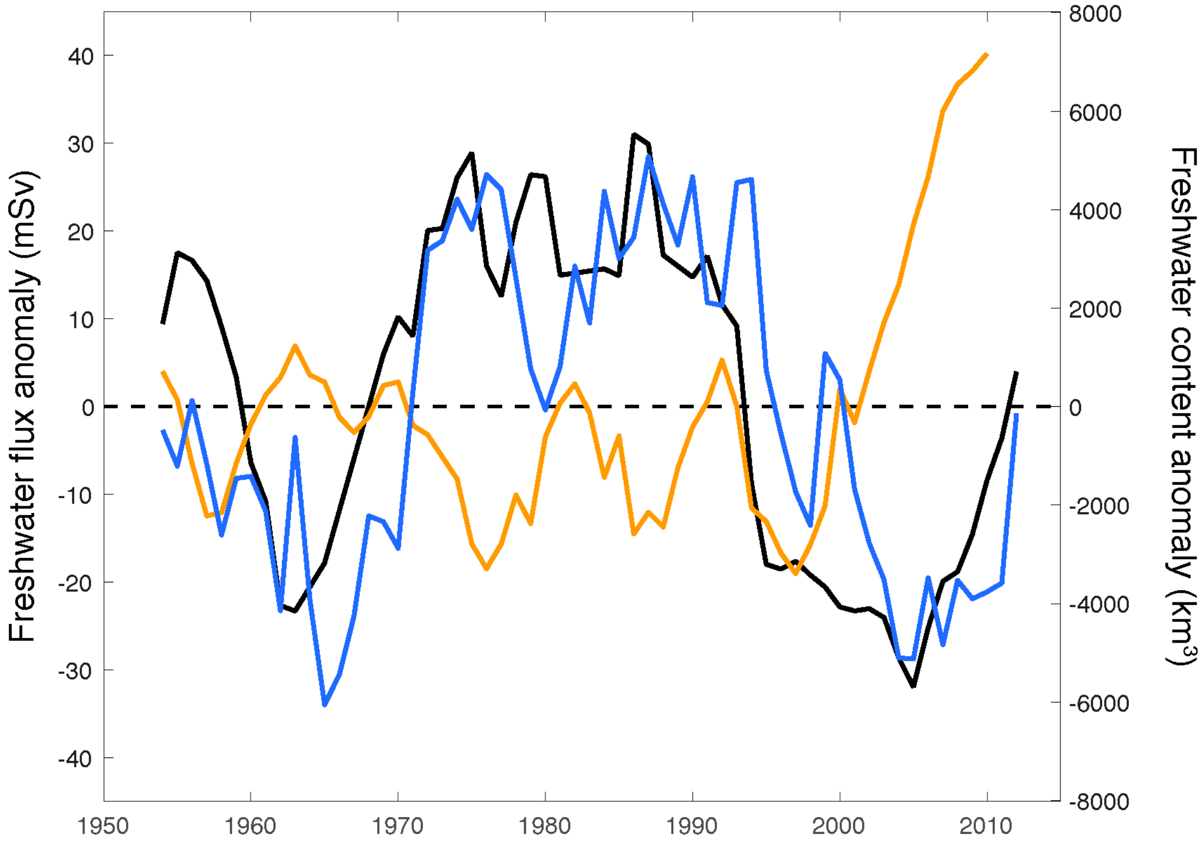

Figure 9. Arctic freshwater export flux anomaly (mSv; Seal Island LC-Arctic flux anomaly using 0 ºC CIL definition, 7-year running average, as Figure 9b; black); Subpolar North Atlantic freshwater content (FWC; km^3) anomaly (blue); Arctic FWC anomaly from Polyakov et al. (2013) as a 7-year running average (orange).

1168

Downloaded from http://journals.ametsoc.org/jcli/article-pdf/doi/10.1175/JCLI-D-19-0083.1/4954456/jclid190083.pdf by UNIVERSITY OF SOUTHAMPTON HIGHFIELD user on 11 June 2020

Accepted for publication in *Journal of Climate*. DOI10.1175/JCLI-D-19-0083.1.